

## COMPARATIVE ANALYSIS OF NANO FLUIDS USED FOR HEAT TRANSFER APPLICATIONS

Lalit Makhan Mishra<sup>1</sup>; Mohit Maheshwarkar<sup>2</sup>

<sup>1</sup>Research Scholar; <sup>2</sup> Associate Professor

Department of Mechanical Engineering, Oriental University, Indore (M.P.) INDIA

### Abstract

Present research work is based on the application of different nanofluids and basefluids in an heat exchanger, for the purpose of investigating the best combinations for the application. During the research work, dimensions of a standard shell and heat exchanger were adopted from a customized machine manufacturing firm, and with the help simulation approach, maximum heat flux, enthalpy drop at exit and exit temperature were calculated for different combinations of basefluids and nanofluids, as well as basefluids. For this purpose, ANSYS 2021 R1 software was used, and conjugate heat transfer approach with k-epsilon model was adopted. In order to get a unique result, a statistical technique, relative standard deviation, was also used. The basefluids used were, water and ethylene glycol, whereas the nanofluids used were Al, Al<sub>2</sub>O<sub>3</sub>, Cu, CuO, MgO, MWCNT, NiO, SiO<sub>2</sub>, TiO<sub>2</sub>. The results of the research work showed that the combination H<sub>2</sub>O-NiO showed the best performance, and H<sub>2</sub>O was considered as the best basefluid.

**Keywords:** Nanofluids, basefluids, ANSYS 2021 R1, heat transfer, k-epsilon model, heat exchanger.

### 1. Introduction

Techniques to improve heat transmission are crucial for energy conservation and the use of the best energy sources. It is the process of raising a heat transfer system's efficiency (Gugulothu et al., 2017a). Gugulothu et al. (2017b) also state that during the past few decades, heat transfer enhancement technology has been created and is now often used in heat exchanger applications in the industrial, chemical, and automotive industries. In many industrial processes, working fluids are heated or cooled using heat exchangers. According to Nivedini et al. (2020), a heat exchanger can be used to transfer heat energy from one channel to another.

A lot of work has been done in recent years to develop affordable strategies for enhancing heat exchanger performance (Gugulothu et al., 2017b). Nanofluids have reportedly been investigated as a novel alternative fluid solution to improve the effectiveness and profitability of thermal systems in industrial, commercial, and residential applications. Considering these facts, present research paper is devoted to the investigations on the performance evaluation of different combinations of nanofluids and base fluids in a shell and tube heat exchanger.

#### 1.1 Objectives of the Research

Following points represent the objectives of proposed research work:

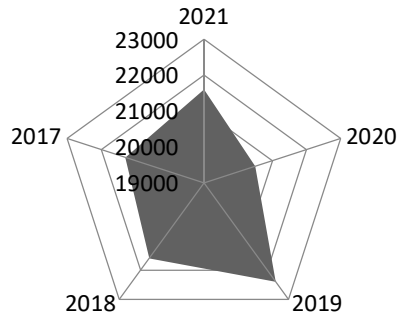
- a) Investigations of thermal properties of an heat exchanger with nanofluids;
- b) Ranking of nanofluids in regard to their suitability in the heat exchanger.

## 2. Literature Review

Present section is devoted to different aspects of contributions of researchers in the field of research on nanofluids, base fluids as well as heat exchangers and concludes with the investigated gaps in the research.

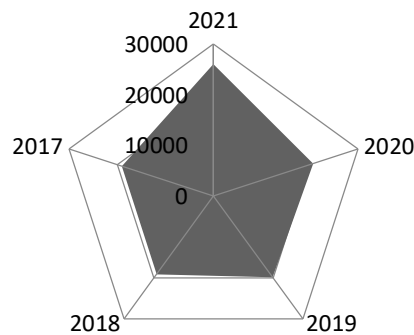
### 2.1 Research on Heat Exchangers and Nanofluids

Figure 2.1 shows the radar graph for the research publications containing the terms heat exchanges in last five years.



**Figure 2.1: Radar Graph on Publications containing the terms Heat Exchangers in last five years**

Figure 2.2 shows the radar graph for the research publications containing the terms heat exchanges and nano fluids in last five years.



**Figure 2.2: Radar Graph on Publications containing the terms Heat Exchangers and Nano Fluids in last five years**

### 2.2 Contributions of Researchers in the field of Heat Exchangers with Nanofluids

Table 2.1 shows some of the selected research contributions of Indian researchers in last five years.

**Table 2.1: Research Contributions of Indian Researchers in last five years**

| S. No | Reference                    | Research Contribution   |
|-------|------------------------------|---|
| 1.    | Reddy et al. (2021)          | thermodynamic analysis of tubular heat exchanger with water and Nano- fluid mixture as a working fluid with different concentration of Nano particles           |
| 2.    | Issa (2021)                  | A Review on Thermophysical Properties and Nusselt Number Behavior of Al <sub>2</sub> O <sub>3</sub> Nanofluids in Heat Exchangers                               |
| 3.    | Sridhar et al. (2021)        | Study of enhancement in heat transfer for a Shell and Tube Heat Exchanger Using SnO <sub>2</sub> -Water and Ag-Water Nanofluids                                 |
| 4.    | Malika et al. (2021)         | Simulation study of a low volume fraction CuO–ZnO/water hybrid nanofluid in a shell and tube heat exchanger   |
| 5.    | Ahmad Ghozatloo (2021)       | Convective heat transfer enhancement of graphene nanofluids in shell and tube heat exchanger  |
| 6.    | Chupradit et al. (2021)      | Use of Organic and Copper-Based Nanoparticles on the Turbulator Installment in a Shell Tube Heat Exchanger  |
| 7.    | Rajput et al. (2021)         | Enhancement of Nusselt number by using Al <sub>2</sub> O <sub>3</sub> and TiO <sub>2</sub> Nanofluids in Heat Exchangers  |
| 8.    | Kanti et al. (2020)          | Application of fly ash as a nano fluid in heat transfer applications  |
| 9.    | Salari et al. (2020)         | Experimentation on forced convection heat transfer of a nanofluid in a heat exchanger filled with partially porous material                                     |
| 10.   | Chaurasia and Sarviya (2020) | CuO/water nano - fluid was used as a working fluid and compared with water  |
| 11.   | Nivedini et al. (2020)       | Enhancement of thermal energy transfer by the usage of nanofluid instead of the conventional fluid  |
| 12.   | Sathish et al. (2020)        | Study on temperature difference of aluminium nitride nanofluid used in solar flat plate collector over normal water   |
| 13.   | Singh and Sarkar (2020)      | Experimentation on hydrothermal characteristics of concentric tube heat exchanger with V-cut twisted tape turbulator using PCM dispersed mono/hybrid nanofluids |

|     |                                |   |
|-----|--------------------------------|---|
| 14. | Bhattad et al. (2020)          | Effect of nanoparticle mixture ratio on Heat transfer characteristics of plate heat exchanger using hybrid nanofluids   |
| 15. | Baskar et al. (2020)           | Analysis the convective heat transfer coefficient characteristics of propanol-based nanofluids for cooling applications   |
| 16. | Radkar et al. (2019)           | The effect of Reynolds number and ZnO nanoparticle on heat transfer coefficient and Nusselt number was examined.  |
| 17. | Kumar et al. (2019)            | Experimentation on characterization of Al nanopowder, synthesis of Al/water nanofluids, and effect of these nanofluids on thermal performance of compact heat exchanger |
| 18. | Rao and Sankar (2019)          | Estimation of convective heat transfer and friction factor of CuO nanofluids flow in a double pipe U-bend heat exchanger under turbulent flow conditions                |
| 19. | Anitha et al. (2019)           | Heat transfer performance (HTP) of hybrid nanofluid is investigated   |
| 20. | Bhanvase et al. (2018)         | Heat transfer enhancement with the use of water based polyaniline nanofluid was investigated in vertical helically coiled tube heat exchanger                           |
| 21. | Naik and Vinod (2018)          | Intensification of heat transfer due to use of non-Newtonian nanofluids in shell and helical coil has been investigated   |
| 22. | Amanuel and Mishra (2018)      | numerical investigation of CuO/water nanofluids in a triple concentric-tube heat exchanger has been carried out using a commercial CFD software                         |
| 23. | Arulprakasajothi et al. (2018) | Performance study of conical strip inserts in tube heat exchanger using water based titanium oxide nanofluid  |
| 24. | Somasekhar et al. (2018)       | A CFD Investigation of Heat Transfer Enhancement of Shell and Tube Heat Exchanger Using Al <sub>2</sub> O <sub>3</sub> -Water Nanofluid                                 |
| 25. | Thakur et al. (2018)           | An Experimental Study of Nanofluids Operated Shell and Tube Heat Exchanger with Air Bubble Injection  |
| 26. | Manikandan and Baskar (2018)   | Heat transfer studies in compact heat exchanger using ZnO and TiO <sub>2</sub> nanofluids in ethylene glycol/water  |
| 27. | Sharma et al. (2017)           | Study of hydrodynamics of CNT nanofluids in helical coils   |
| 28. | Palanisamy & Kumar (2017)      | The heat transfer and pressure drop analysis of a cone helically coiled tube heat exchanger handling Multi  |

|     |                           |   |
|-----|---------------------------|---|
|     |                           | Walled Carbon/water nanofluid carried out experimentally  |
| 29. | Gugulothu et al. (2017a)  | Study of heat transfer enhancement using passive techniques   |
| 30. | Thakur & Singh (2017)     | Experimentation on heat transfer characteristics of shell and tube heat exchanger was done with the injection of air bubbles at the tube inlet and throughout the tube with water based Al <sub>2</sub> O <sub>3</sub> nanofluids |
| 31. | Barzegarian et al. (2017) | The effect of using Al <sub>2</sub> O <sub>3</sub> -water nanofluid on thermal performance of a commercial shell and tube heat exchanger with segmental baffles assessed experimentally   |

### 2.3 Gaps in the Research and Objectives of Proposed Research

On the basis of the survey of available literature, following research gaps were investigated.

- There is very less research work available which focuses on a broader set of parameters which effect the performance of heat exchanger with nanofluids; and
- Ranking of heat exchangers with nanofluids.

### 3. Solution Methodology

Present section is focuses on the details of equations used for the calculations of properties of nanofluids, model used and software used in the research work, the details of which are presented in upcoming sub-sections.

#### 3.1 Equations used for the Calculations of Properties of Nanofluids

Following equations were used for the calculation of properties of nanofluids (Kleinstreuer and Yu Feng, 2011).

##### a) Density of Nanofluid

Density of the Nanofluid was calculated using following equation:

$$\rho_{nf} = (1 - \varphi) \times \rho_{bf} + \varphi \times \rho_{np} \quad (3.1)$$

.....where,

$\rho_{np}$  = Density of nanoparticles

$\rho_{bf}$  = Density of base fluid

$\varphi$  = Molar concentration of nanoparticles in the base fluid.

##### b) Specific heat of Nanofluid

Specific heat of the Nanofluid was calculated using following equation (Puspitasari et al., 2020):

$$C_{p_{nf}} = (1 - \varphi) \times C_{p_{bf}} + \varphi \times C_{p_{np}} \quad (3.2)$$

.....where,

$C_{p_{nf}}$  = Specific heat of Nanofluid;  
 $C_{p_{bf}}$  = Specific heat of base fluid;  
 $C_{p_{np}}$  = Specific heat of nano-particles;  
 $\varphi$  = Molar concentration of nanoparticles in the base fluid.

### c) Thermal conductivity of Nanofluid

Thermal conductivity of the Nanofluid was calculated using following equation (Puspitasari et al., 2020):

$$\frac{k_{nf}}{k_{bf}} = 1 + \frac{3\left(\frac{k_{np}}{k_{bf}} - 1\right) \times \varphi}{\left(\frac{k_{np}}{k_{bf}} + 2\right) - \left(\frac{k_{np}}{k_{bf}} - 1\right) \times \varphi} \quad (3.3)$$

.....where,

$k_{np}$  = Density of nanoparticles

$k_{bf}$  = Density of base fluid

$\varphi$  = Molar concentration of nanoparticles in the base fluid.

### d) Viscosity of Nanofluid

Viscosity the Nanofluid was calculated using following equation (Colla et al., 2012):

$$\mu_{nf} = \mu_{bf} \times (1 + 2.5 \times \varphi + 6.5 \times \varphi^2) \quad (3.4)$$

.....where,

$\mu_{nf}$  = Viscosity of nanofluid

$\mu_{bf}$  = Viscosity of base fluid

$\varphi$  = Molar concentration of nanoparticles in the base fluid.

## 3.2 Model used in the Research Work

The model used in the research work was k-epsilon model (k- $\epsilon$ ). k-epsilon turbulence model is a very famous model used in the field of computational fluid dynamics for simulating mean flow characteristics for turbulent flow conditions. It is a two equation type of model which offers a general description of existing turbulence by means of two transport equations. Following are the details of variables obtained through k- $\epsilon$  model:

1. The first transported variable is called turbulent kinetic energy (k), which determines the energy in the turbulence; and
2. The second transported variable is used for determining the rate of dissipation of kinetic energy. This variable is called turbulent dissipation ( $\epsilon$ ).

Details of the model are as follows (Mierka *et al.*, 2006):

In the framework of eddy viscosity models, the hydrodynamic behaviour of a turbulent incompressible fluid is governed by the RANS equations for the velocity  $u$  and pressure  $p$ .

$$\frac{\partial u}{\partial t} + u \cdot \nabla u = -\nabla p + \nabla \cdot \left( (V + V_T)[\nabla u + \nabla u^T] \right), \quad \nabla \cdot u = 0 \quad (3.5)$$

where  $\nu$  depends only on the physical properties of the fluid, while  $V_T$  is the turbulent eddy viscosity which is supposed to emulate the effect of unresolved velocity fluctuations  $u'$ . If the standard  $k - \varepsilon$  model is employed, then

$$V_T = C_\mu \frac{k^2}{\varepsilon} \quad (3.6)$$

.....where  $k$  is the turbulent kinetic energy and  $\varepsilon$  is the dissipation rate. Hence, the above system is to be complemented by two additional convection-diffusion-reaction equations for computation of  $k$  and  $\varepsilon$ .

$$\frac{\partial k}{\partial t} + \nabla \cdot \left( ku - \frac{V_T}{\sigma_k} \nabla k \right) = P_k - \varepsilon \quad (3.7)$$

$$\frac{\partial \varepsilon}{\partial t} + \nabla \cdot \left( \varepsilon u - \frac{V_T}{\sigma_\varepsilon} \nabla \varepsilon \right) = \frac{\varepsilon}{k} (C_1 P_k - C_2 \varepsilon) \quad (3.8)$$

.....where

$$P_k = \frac{V_T}{2} |\nabla u + \nabla u^T|^2 \quad (3.9)$$

$k$  and  $\varepsilon$  are responsible for production and dissipation of turbulent kinetic energy, respectively. The default values of the involved empirical constants are as follows:  $C_\mu = 0.09$ ,  $C_1 = 1.44$ ,  $C_2 = 1.92$ ,  $\sigma_k = 1.0$ ,  $\sigma_\varepsilon = 1.3$ .

### 3.3 Software used in the Research Work

Software used in the research work was ANSYS 2021 R1. ANSYS is a very popular analysis tools, developed by ANSYS Inc., USA for simulating problems of structural analysis, thermal analysis, computational fluid dynamics, modal analysis, harmonic analysis, transient dynamics, buckling, and other categories. The software also offers the facility to develop simple models. With the help of inbuilt library, one can find out the properties of materials. ANSYS also include a set of models to solve complex problems of engineering, sciences, and other applications. Following are the salient features of the software:

- Provides excellent simulation facility;
- Offers different types of complex analysis like modal, transient, etc;
- Provides different approaches to solve a problem with different inbuilt models;
- Facilitates in modeling of simple parts;
- Inbuilt library for properties of materials;
- Separate modules for different analyses purposes like structural, modal, etc; and
- Better graphics facilities.

## 4. Case Study

Present section details of problem formulation and solution, the details of which are presented in upcoming sub-sections.

### 4.1 Problem Formulation

Based on the survey of literature the following problem was formulated:

### Comparative Analysis of Nano Fluids used for Heat Transfer Applications

### 4.2 Solution of the Problem

Following steps were undertaken in order to solve the research problem:

- a) First of all a model of shell and tube heat exchanger was created with the following dimensions (as obtained from a customized machine making firm:
  - Diameter of shell=1 meter;
  - Length of shell and tube=4 meters;
  - Distance of centers of hot fluid ends from both the end faces=0.5 m;
  - Distance between hot fluid pipe ends from the surface of shell=0.8 m;
  - Diameters of hot fluid pipes=0.3 m;
  - Diameter of tube=0.2 m;
  - Extursion of tube from the surface of shell in both sides=0.5 m; and
  - Material of shell and tube=copper.
- b) In the next step, from above dimensions, a model of heat exchanger was created, in ANSYS2021R1, as shown below:

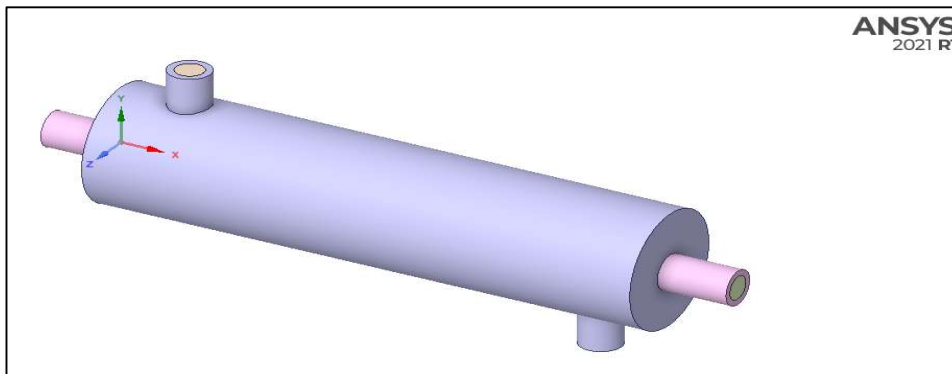


**Figure 4.1: Model of Shell and tube Heat Exchanger**

- c) In the next step of research work, meshing of the generated model was performed, in order to make the body deformable. Figure 5.2 shows the meshed model of heat exchanger.



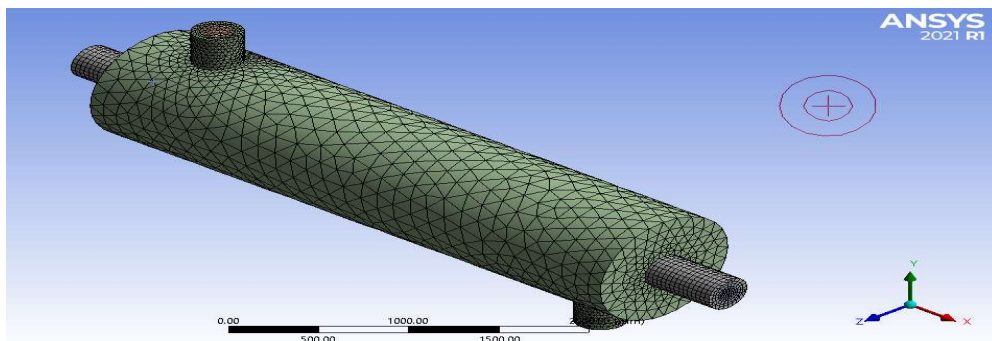


**Figure 4.2: Meshed Model of the Heat Exchanger**

Table 4.1 represents the meshing statistics for the heat exchanger.

**Table 4.1: Mesh Statistics for the Heat Exchanger**

| S. No | Parameter               | Value       |
|-------|-------------------------|-------------|
| 1.    | Type of mesh            | Conformal   |
| 2.    | Type of meshing element | Tetrahedron |
| 3.    | Number of nodes         | 86.2k       |
| 4.    | Number of elements      | 4263.2k     |

d) In the next, the properties of nano particles and base fluids were investigated form the survey of available literature, as follows.

**Table 4.2: Properties of Base Fluids and Nano Particles**

(Kleinstreuer and Yu Feng, 2011; Puspitasari et al., 2020; Colla et al. 2012)

| S. No | Material                       | Density (kg m <sup>-3</sup> ) | Specific Heat (J kg <sup>-1</sup> K <sup>-1</sup> ) | Thermal Conductivity (W m K <sup>-1</sup> ) |
|-------|--------------------------------|-------------------------------|---|---|
| 1.    | Water                          | 996                           | 4178  | 0.615                                       |
| 2.    | Ethylene Glycol                | 1110                          | 2360  | 0.254                                       |
| 3.    | Al <sub>2</sub> O <sub>3</sub> | 3970                          | 775   | 39  |
| 4.    | TiO <sub>2</sub>               | 4000                          | 711   | 8.04  |
| 5.    | CuO                            | 6500                          | 525   | 17.65                                       |
| 6.    | NiO                            | 6670                          | 603   | 46.024                                      |
| 7.    | Cu                             | 8933                          | 385   | 400   |
| 8.    | Al                             | 2800                          | 900   | 235   |
| 9.    | MgO                            | 3580                          | 918   | 42  |
| 10.   | SiO <sub>2</sub>               | 2200                          | 745   | 1.4   |
| 11.   | MWCNT                          | 1700–2100                     | 1200  | 2000  |

e) In next step, properties of nanofluids were calculated, by using equations provided in last unit, form the properties of nanoparticles and base fluids, as shown below.

**Table 4.3: Properties of Nanofluids**

| S. No | Nanofluid  | Density (kg m-3) | Specific Heat (J kg-1 K-1) | Thermal Conductivity (W m K-1) | Viscosity (N s/m <sup>2</sup> , Pa s) |
|-------|--|------------------|----------------------------|--------------------------------|---------------------------------------|
| 1.    | H <sub>2</sub> O- SiO <sub>2</sub>               | 1116.4           | 3834.7                     | 0.671763668                    | 0.001047                              |
| 2.    | EGO- SiO <sub>2</sub>                            | 1219             | 2198.5                     | 0.302693                       | 0.021254                              |
| 3.    | H <sub>2</sub> O -MVCNT                          | 1066.4           | 3880.2                     | 0.81979                        | 0.001047                              |
| 4.    | EG -MVCNT  | 1169             | 2244                       | 0.338631                       | 0.021254                              |
| 5.    | H <sub>2</sub> O -Al                             | 1176.4           | 3850.2                     | 0.818223                       | 0.001047                              |
| 6.    | Eg -Al   | 1279             | 2214                       | 0.338362                       | 0.021254                              |
| 7.    | H <sub>2</sub> O-MgO                             | 1254.4           | 3852                       | 0.810325                       | 0.001047                              |
| 8.    | Eg -MgO  | 1357             | 2215.8                     | 0.336984                       | 0.021254                              |
| 9.    | H <sub>2</sub> O                                 | 996              | 4178                       | 0.615                          | 0.000798                              |
| 10.   | Eg   | 1110             | 2360                       | 0.254                          | 0.0162                                |
| 11.   | H <sub>2</sub> O -TiO <sub>2</sub>               | 1296.4           | 3831.3                     | 0.775637                       | 0.001047                              |
| 12.   | Eg -TiO <sub>2</sub>                             | 1399             | 2195.1                     | 0.330363                       | 0.021254                              |
| 13.   | H <sub>2</sub> O -Al <sub>2</sub> O <sub>3</sub> | 1293.4           | 3837.7                     | 0.809607                       | 0.001047                              |
| 14.   | Eg -Al <sub>2</sub> O <sub>3</sub>               | 1396             | 2201.5                     | 0.336856                       | 0.021254                              |
| 15.   | H <sub>2</sub> O -CuO                            | 1546.4           | 3812.7                     | 0.79798                        | 0.001047                              |
| 16.   | Eg- CuO  | 1649             | 2176.5                     | 0.334737                       | 0.021254                              |
| 17.   | H <sub>2</sub> O -Cu                             | 1789.7           | 3798.7                     | 0.818953                       | 0.001047                              |
| 18.   | Eg Cu  | 1892.3           | 2162.5                     | 0.338488                       | 0.021254                              |
| 19.   | H <sub>2</sub> O -Nio                            | 1563.4           | 3820.5                     | 0.811144988                    | 0.001047                              |
| 20.   | Eg -Nio  | 1666             | 2184.3                     | 0.337128924                    | 0.021254                              |

f) In the next step of the research work, meshed model was solved using k-epsilon model, keeping realizable and scalable wall functions ON. Energy equation was also ON. During the analysis, following boundary conditions were used, with the help of an expert's opinion:

- Hot inlet = Velocity inlet;
- Cold inlet = Velocity inlet;
- Inlet velocity of hot fluid = 1 m/sec
- Temperature of hot fluid = 100°C;
- Inlet velocity of cold fluid = 1 m/sec; and
- Temperature of cold fluid = 20°C.

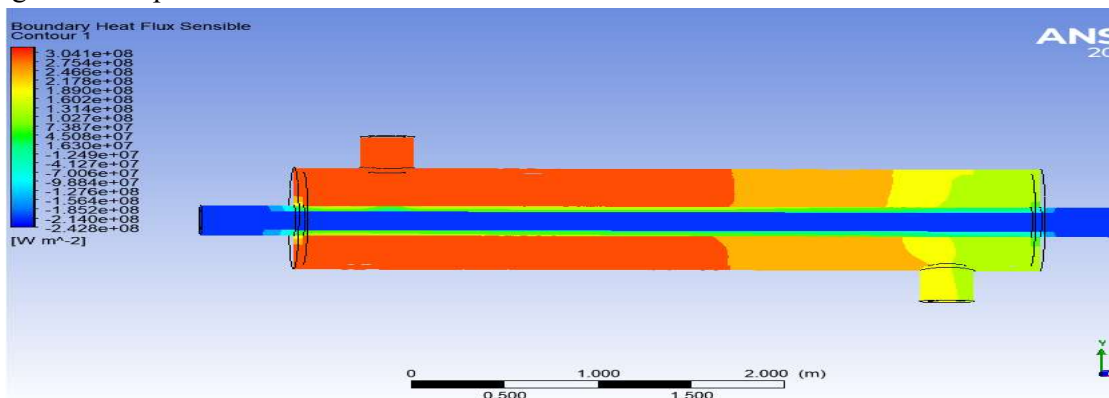
g) In the next step, solution was in hybrid mode with 100 iterations, and after that contours of results were drawn.

## 5. Results and Discussion

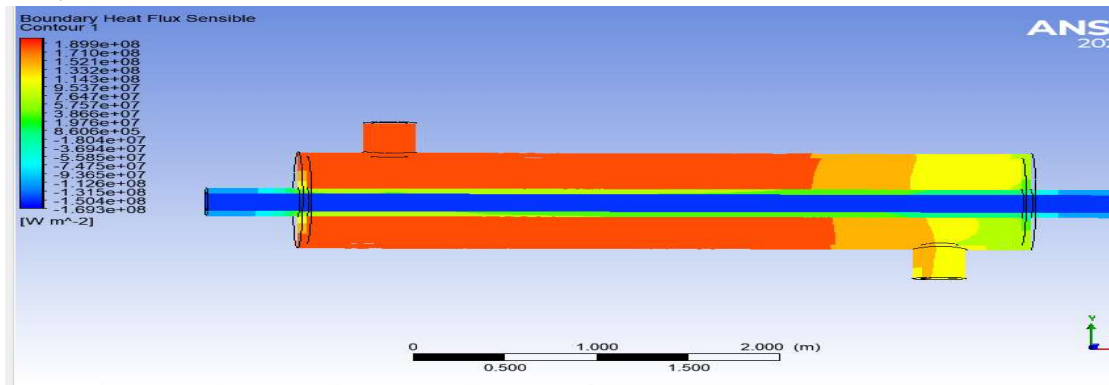
Present section is devoted to the results obtained from the research work, and discussion made about the research, the details of which are presented in upcoming sub-sections.

### 5.1 Results

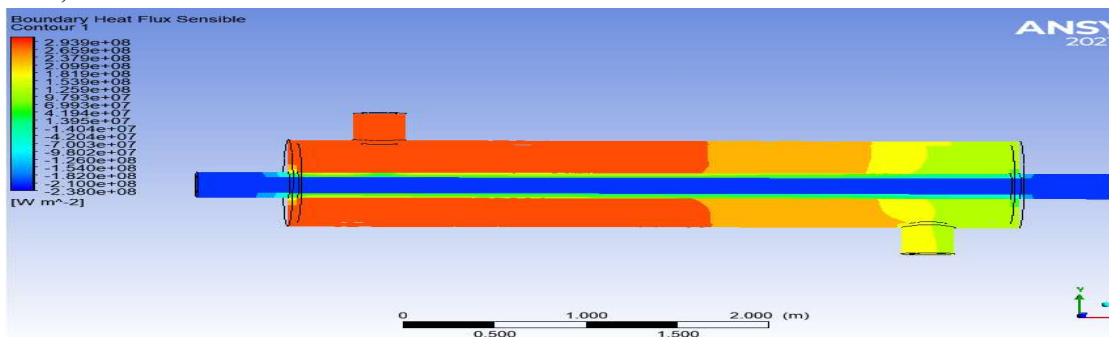
Figures 5.1 represents the results obtained for maximum heat flux.



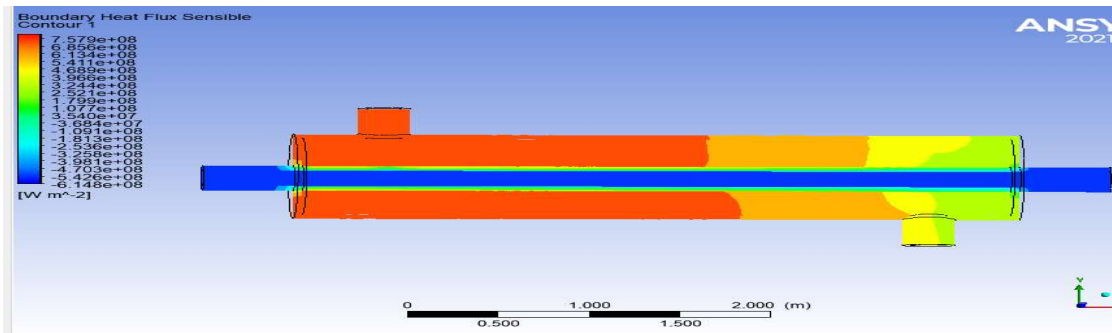
a) H<sub>2</sub>O-SiO<sub>2</sub>



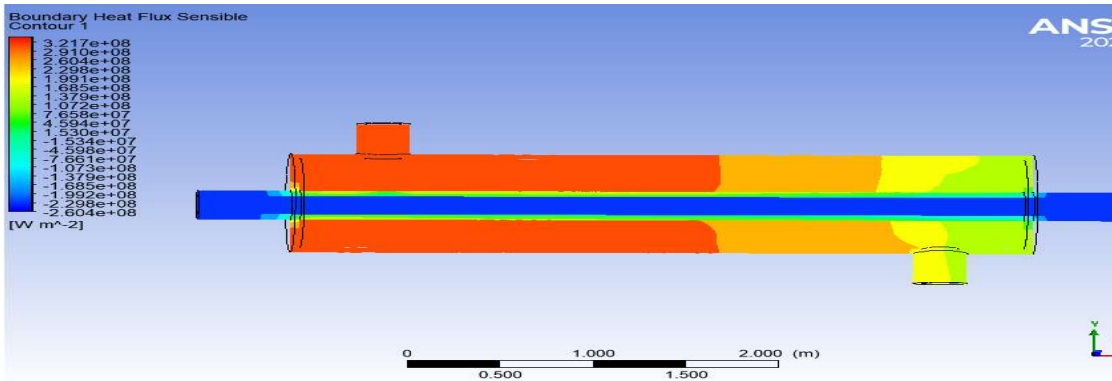
b) EG-SiO<sub>2</sub>



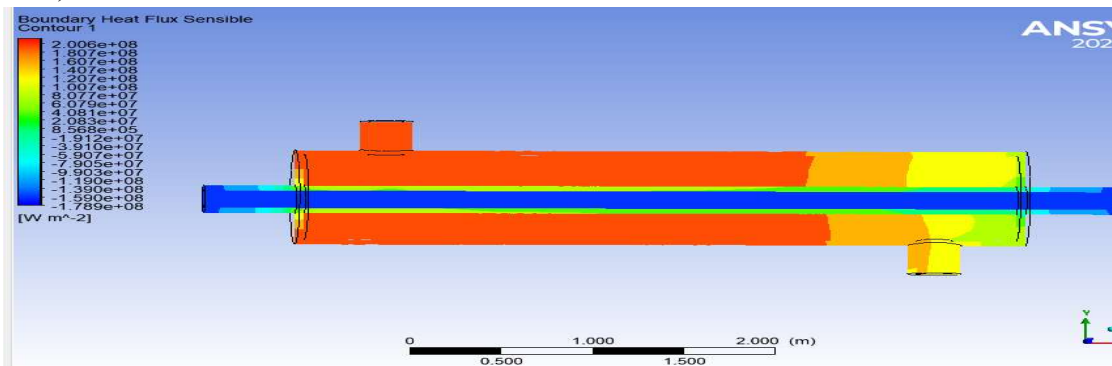
c) H<sub>2</sub>O-MVCNT



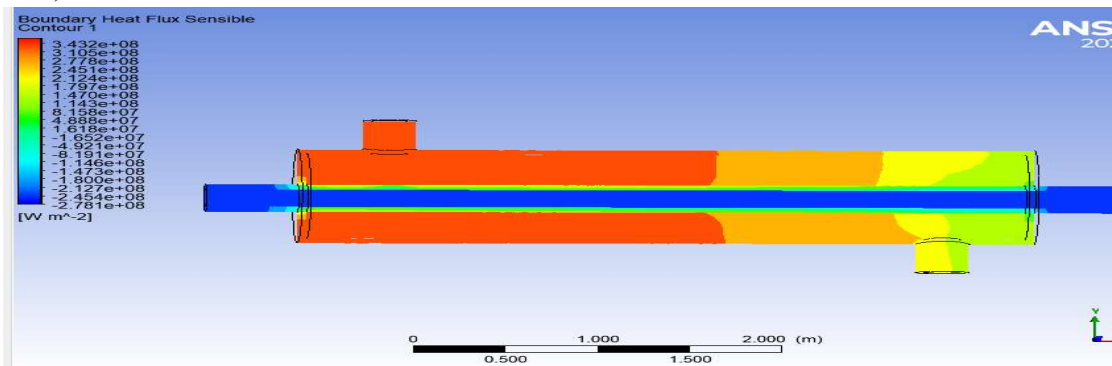
d) EG-MVCNT



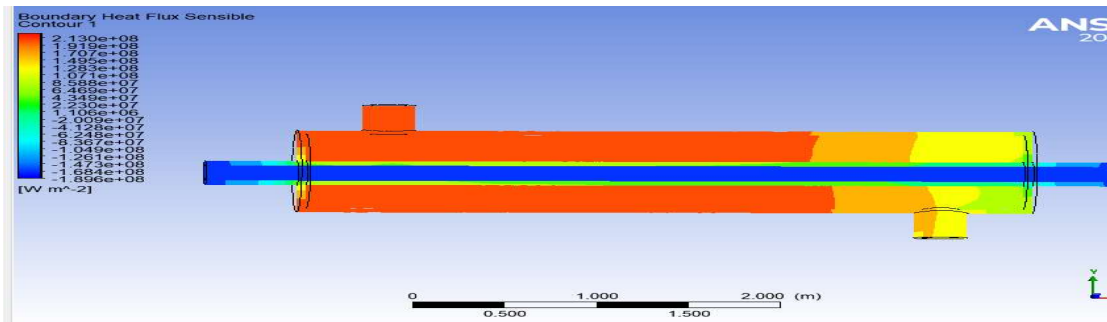
e) H<sub>2</sub>O-Al



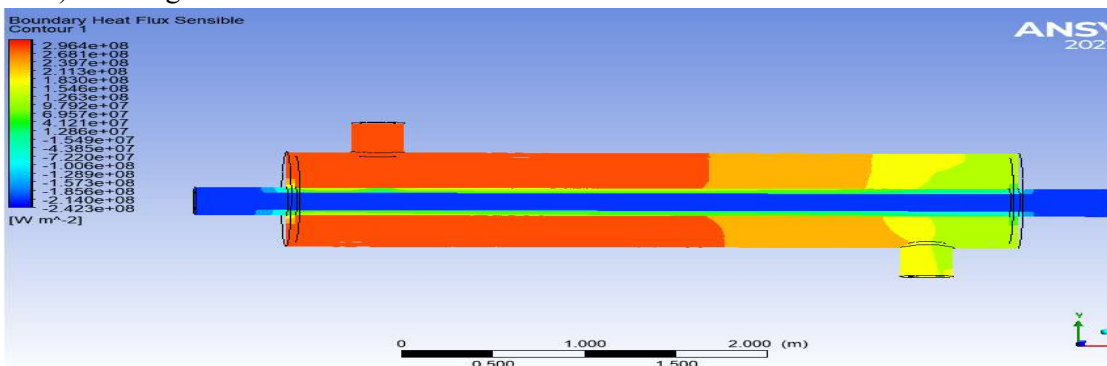
f) EG-Al



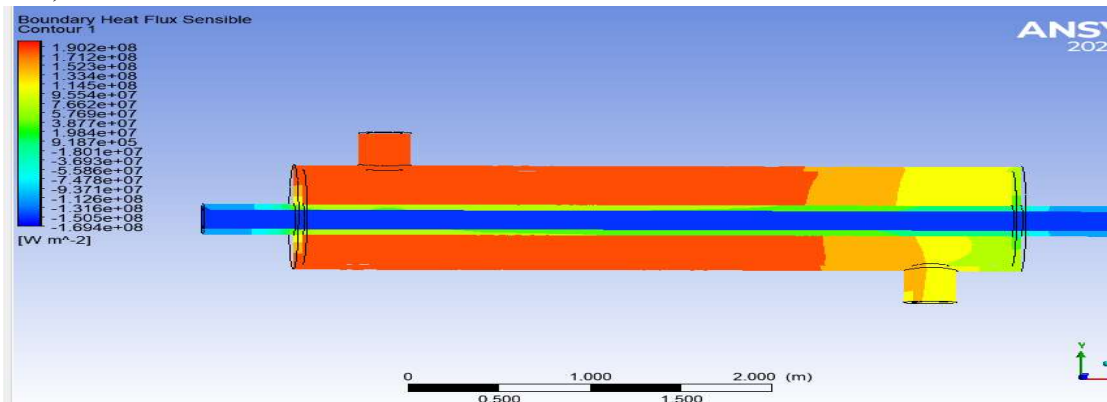
g) H<sub>2</sub>O-MgO



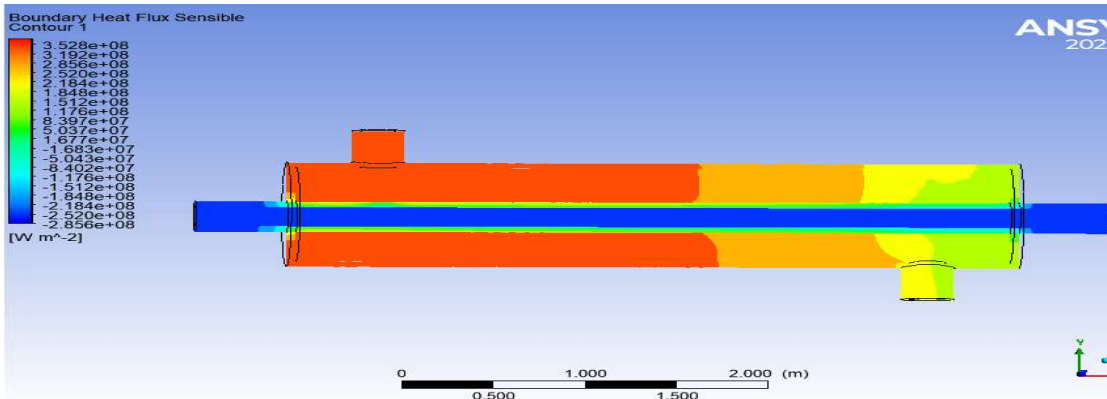
h) EG-MgO



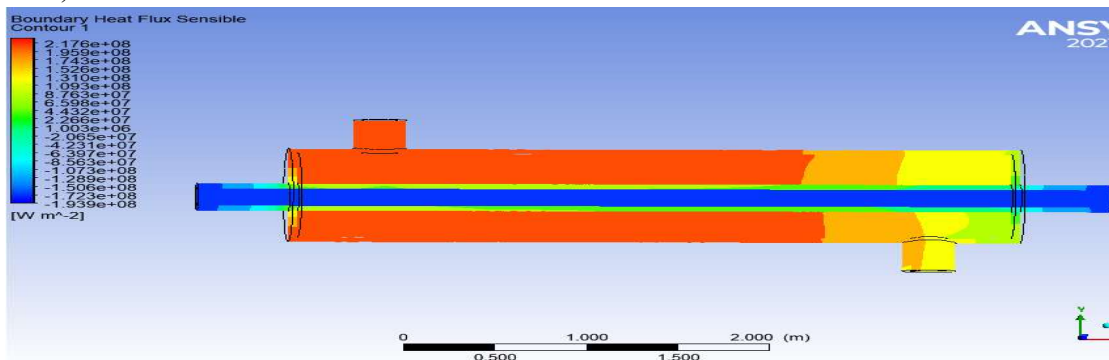
i) H<sub>2</sub>O



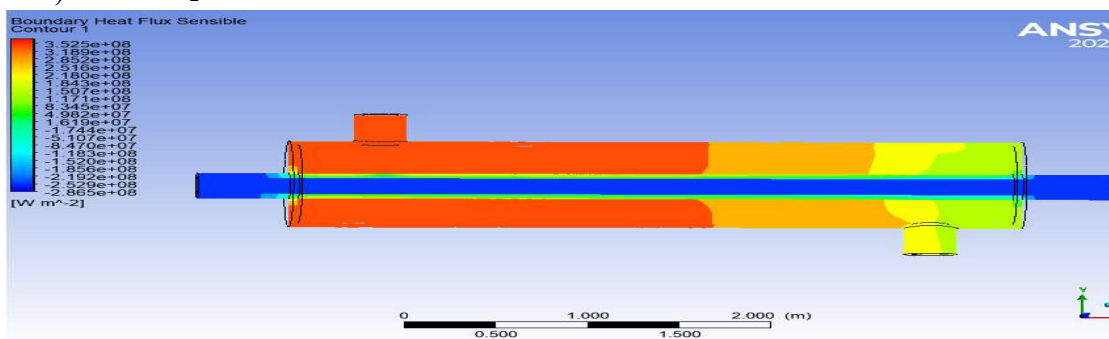
j) EG



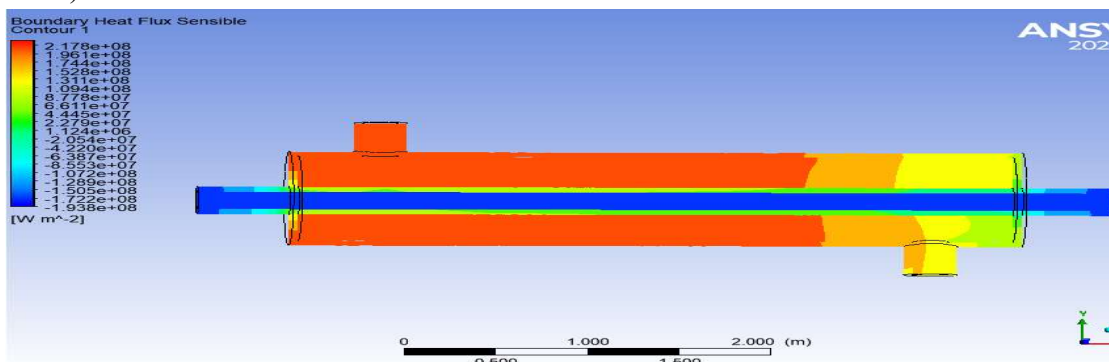
k) H<sub>2</sub>O-TiO<sub>2</sub>



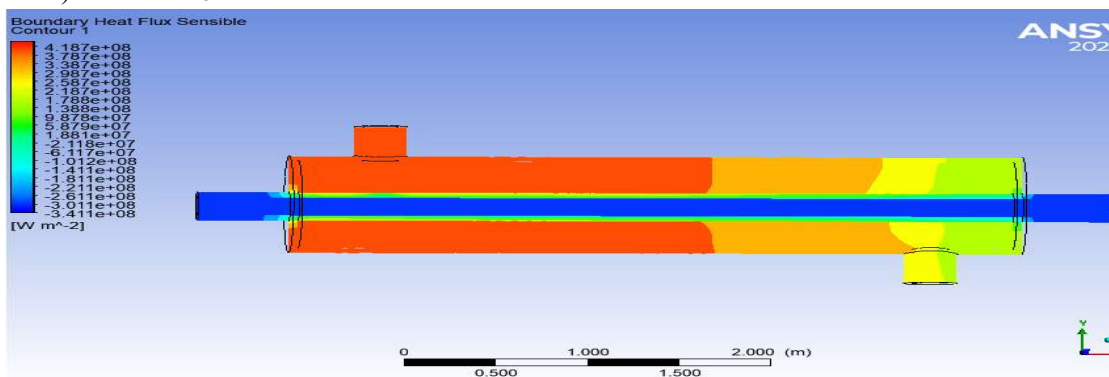
l) EG-TiO<sub>2</sub>



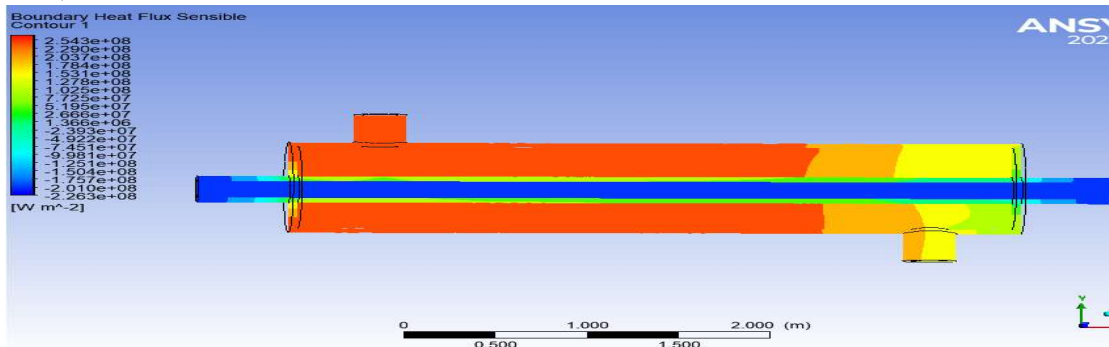
m) H<sub>2</sub>O-Al<sub>2</sub>O<sub>3</sub>



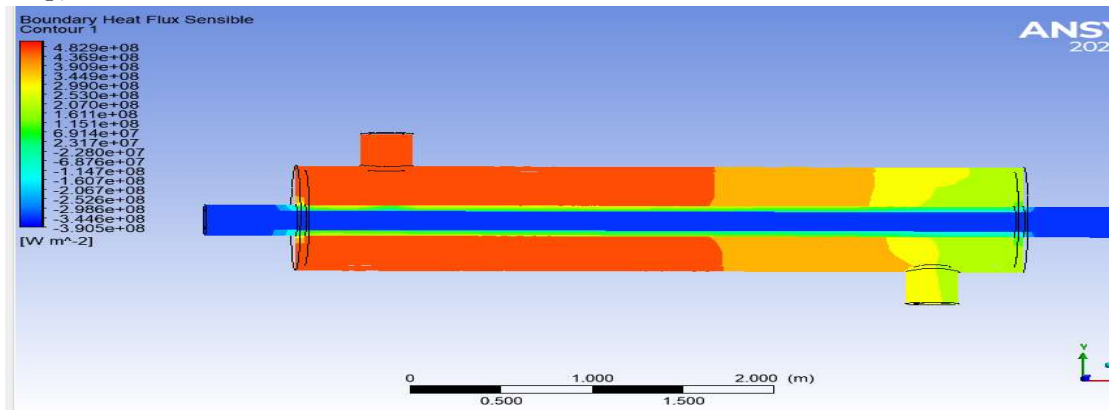
n) EG-Al<sub>2</sub>O<sub>3</sub>



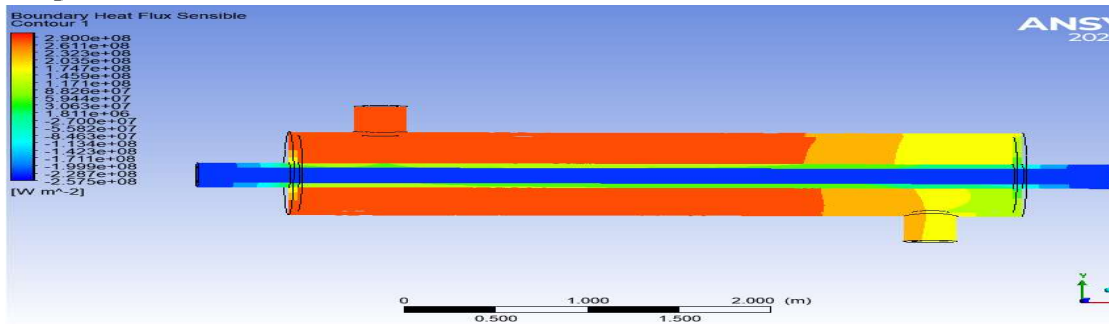
o) H<sub>2</sub>O-CuO



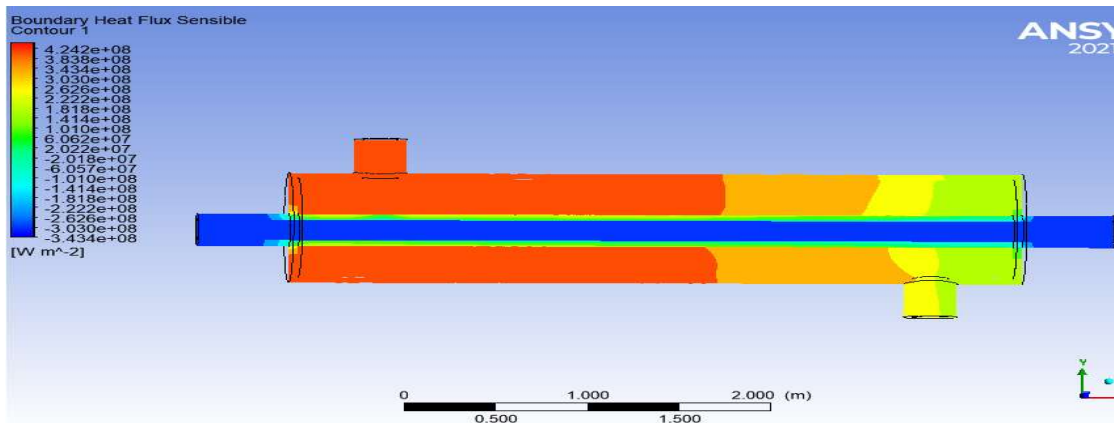
p) EG-CuO



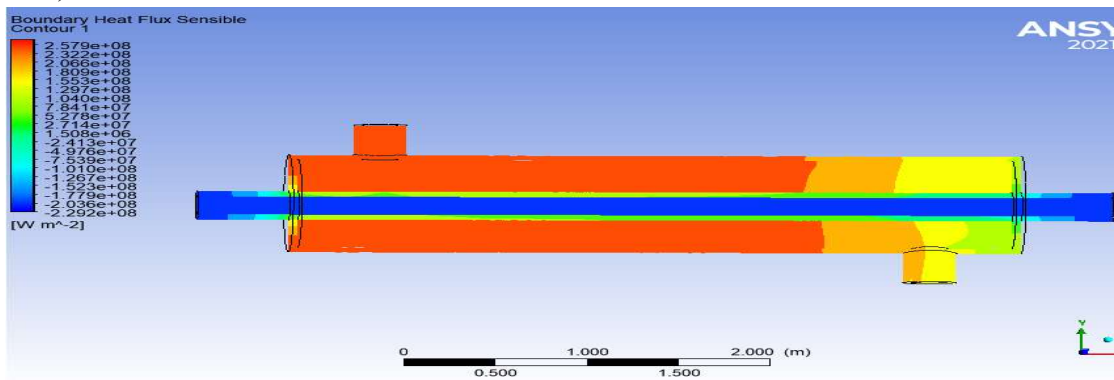
q) H<sub>2</sub>O-Cu



r) EG-Cu



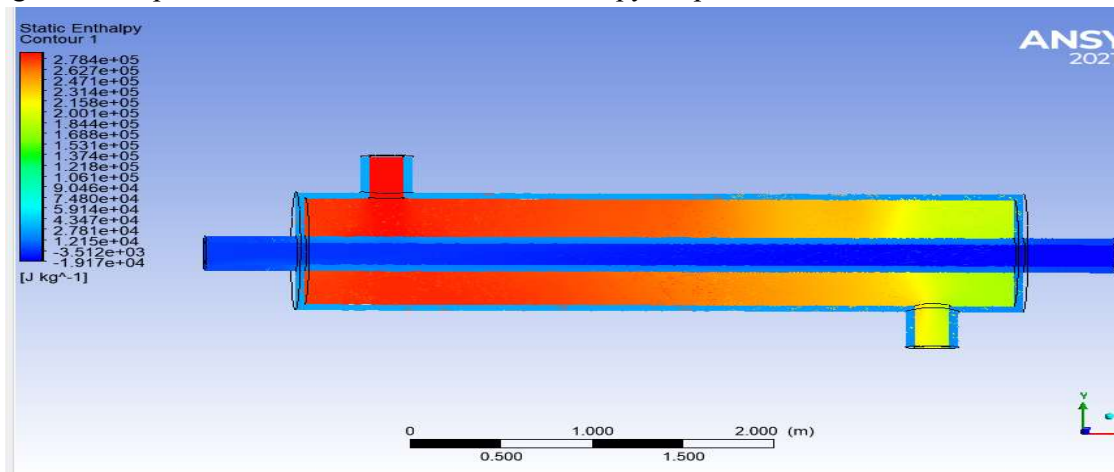
s) H<sub>2</sub>O-NiO



t) EG-NiO

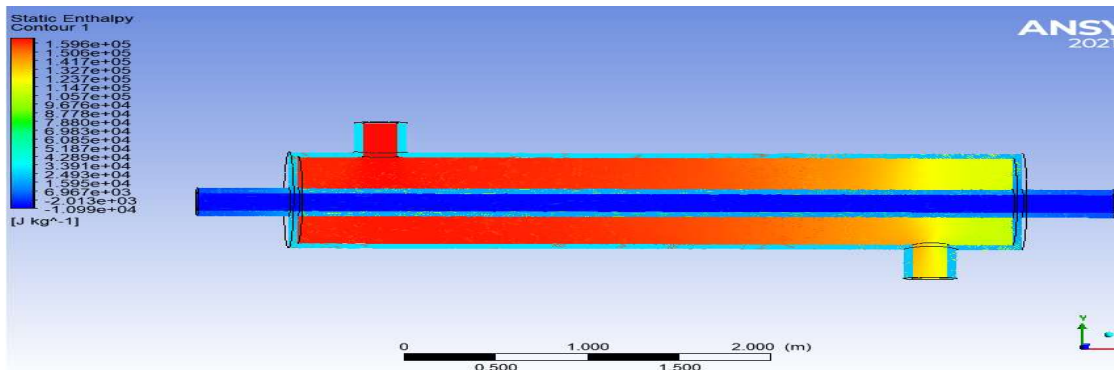
**Figure 5.1: Maximum Heat Fluxes for Different Materials**

Figures 5.2 represents the results obtained for enthalpy drop at exit.

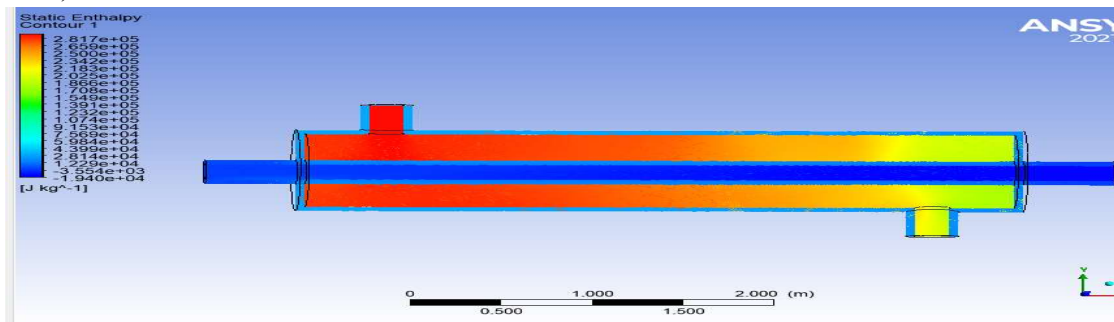


a) H<sub>2</sub>O-SiO<sub>2</sub>

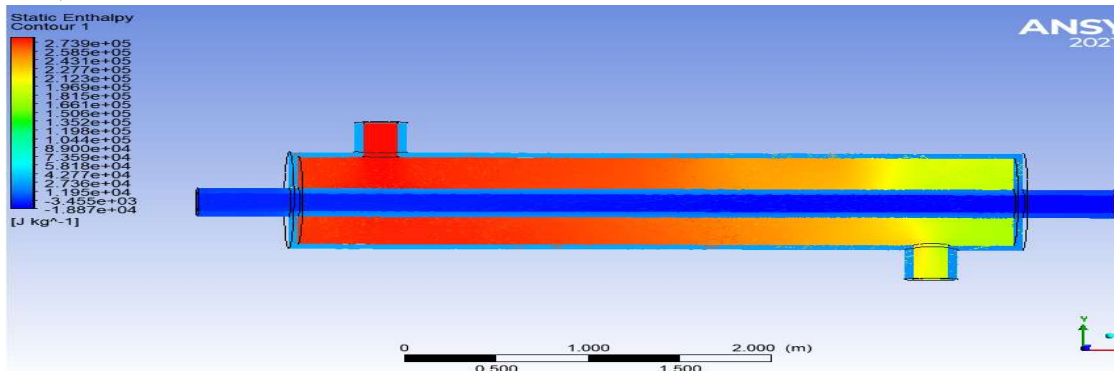




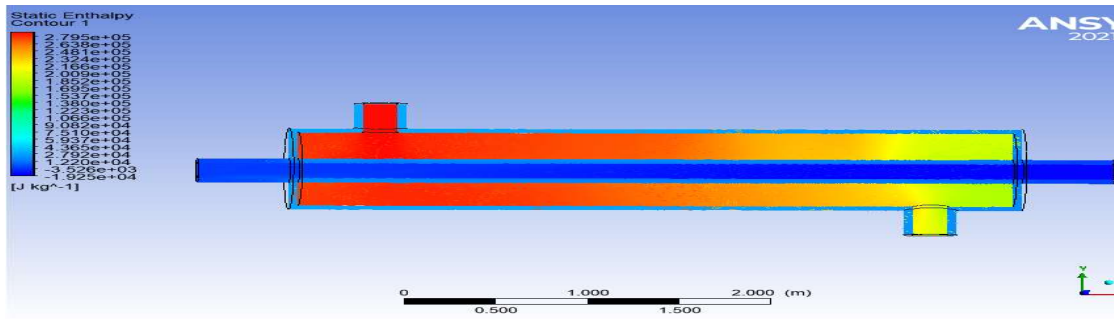
b) EG-SiO<sub>2</sub>



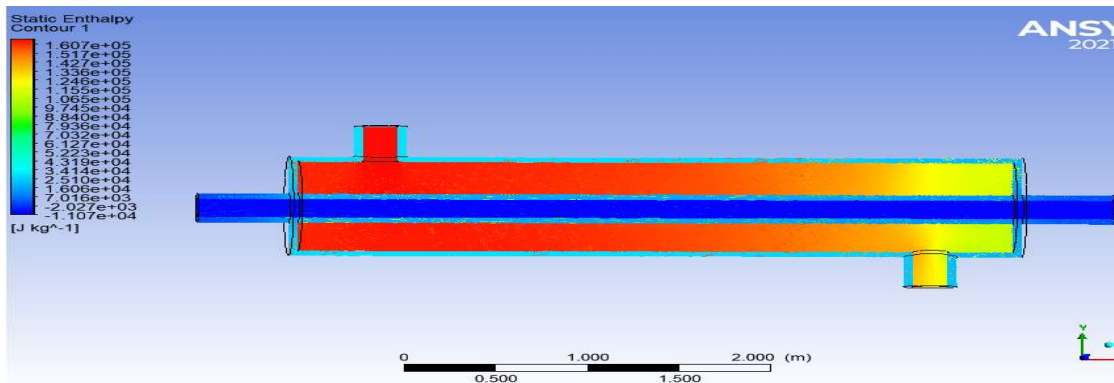
c) H<sub>2</sub>O-MVCNT



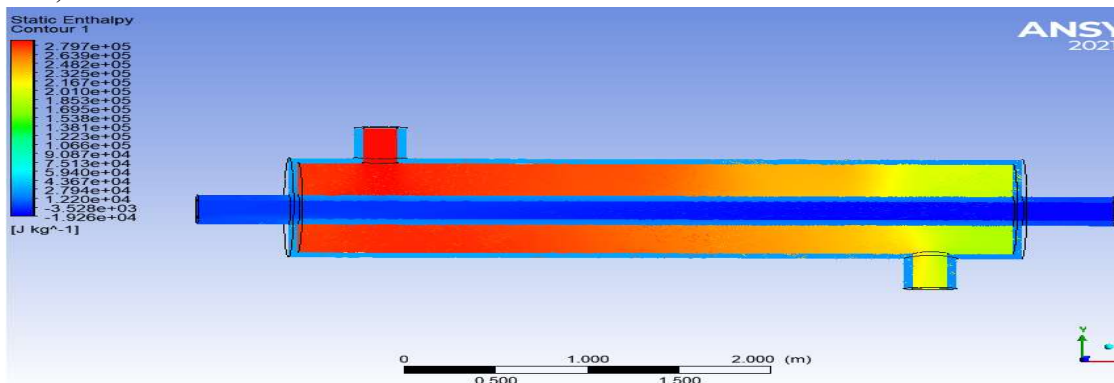
d) EG-MVCNT



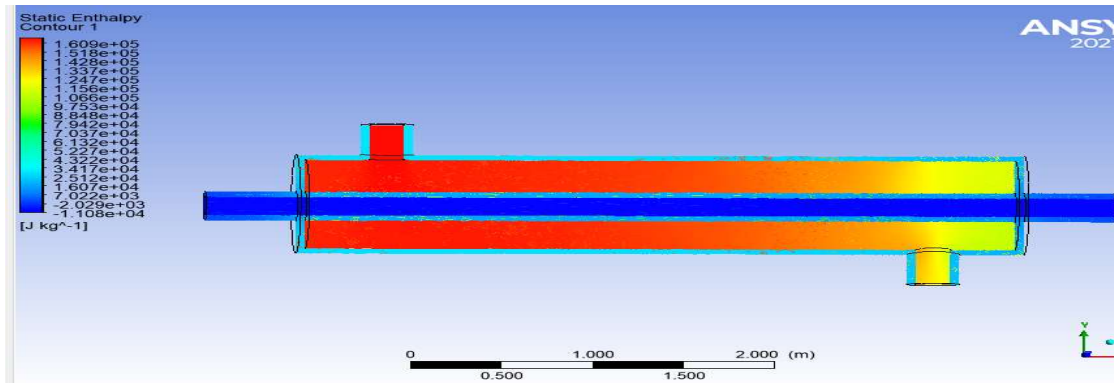
e) H<sub>2</sub>O-Al



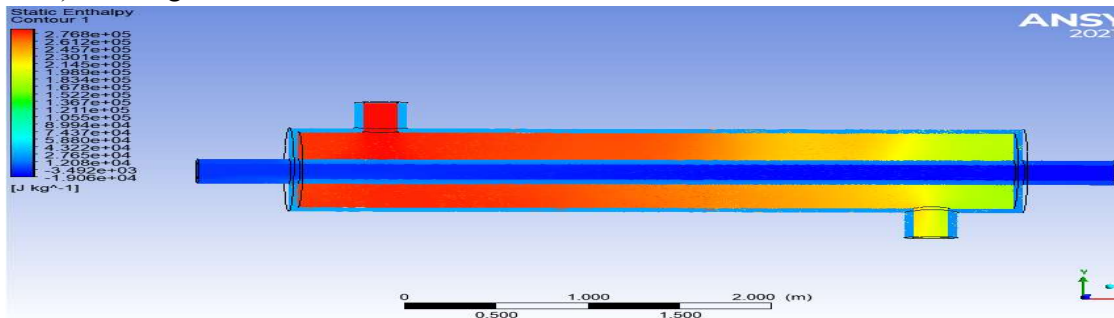
f) EG-Al



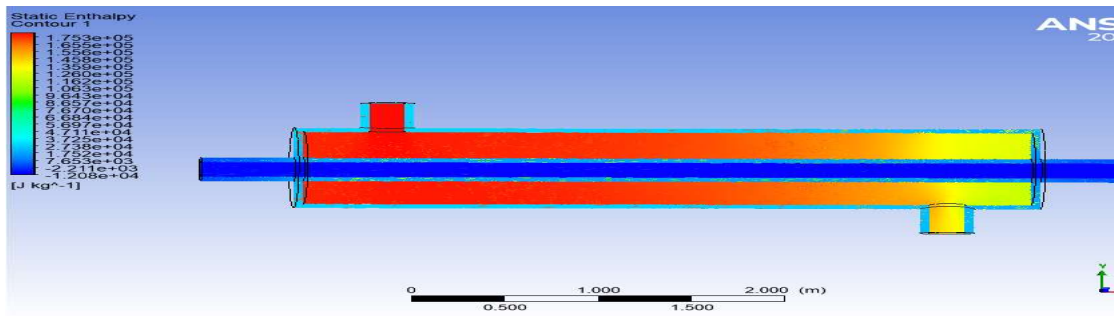
g) H<sub>2</sub>O-MgO



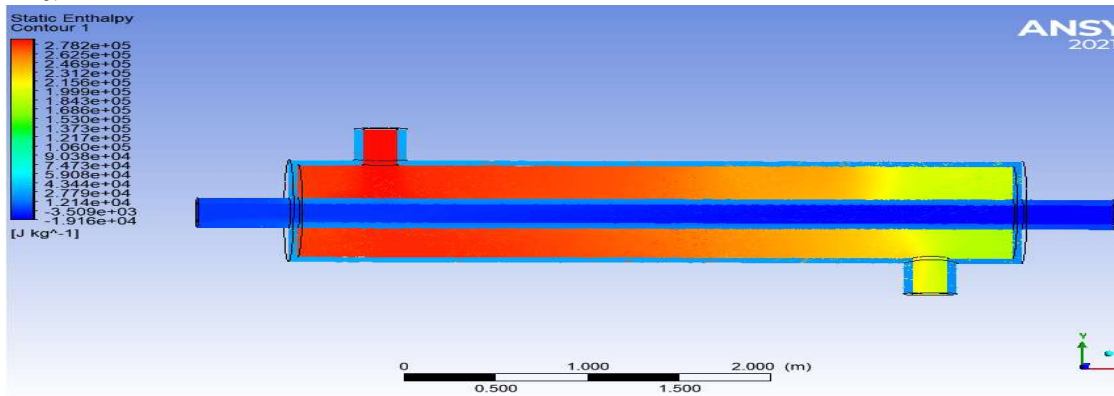
h) EG-MgO



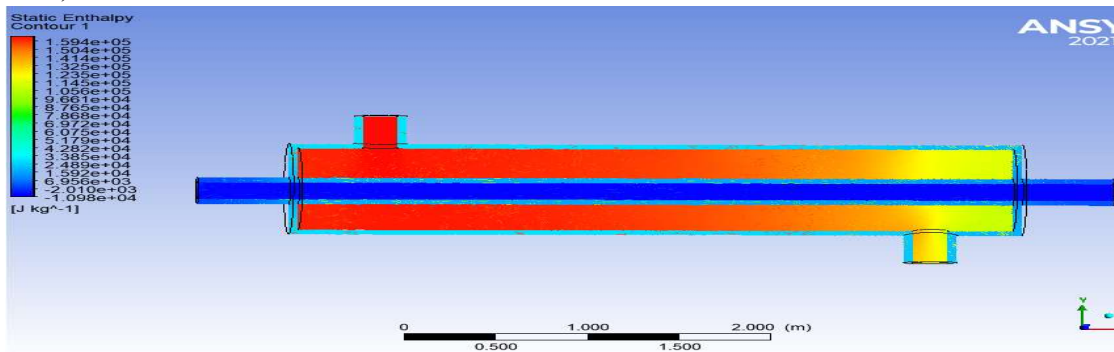
i) H<sub>2</sub>O



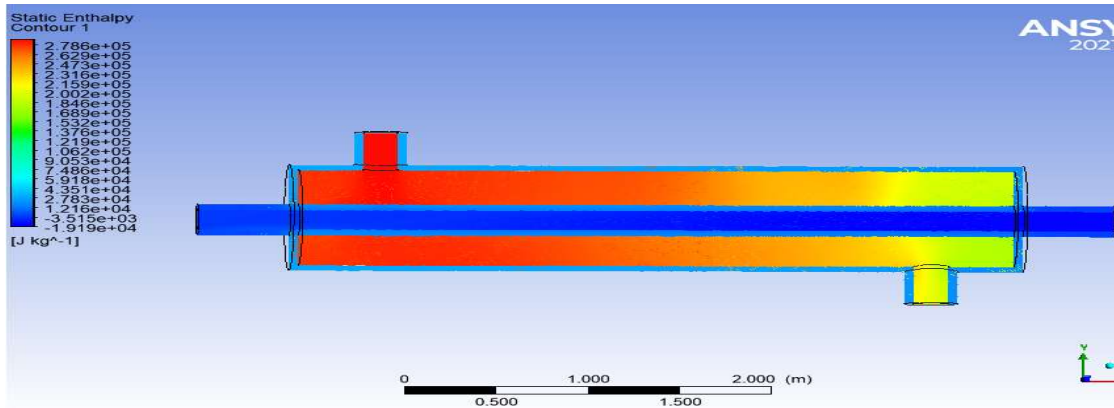
j) EG



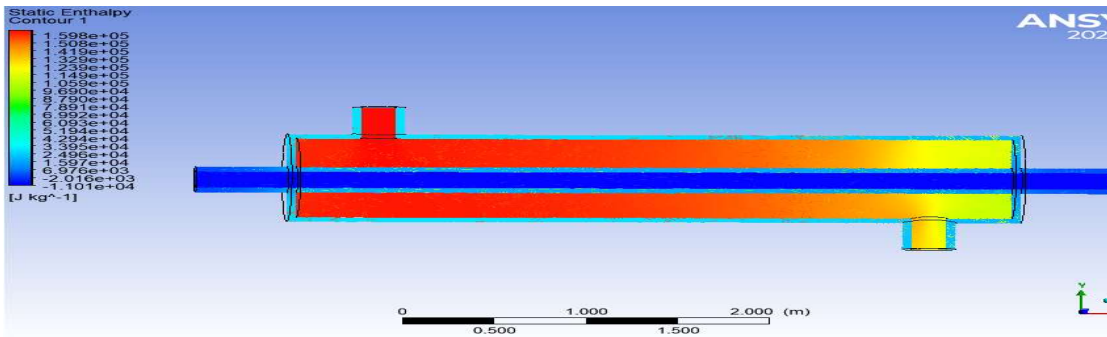
k) H<sub>2</sub>O-TiO<sub>2</sub>



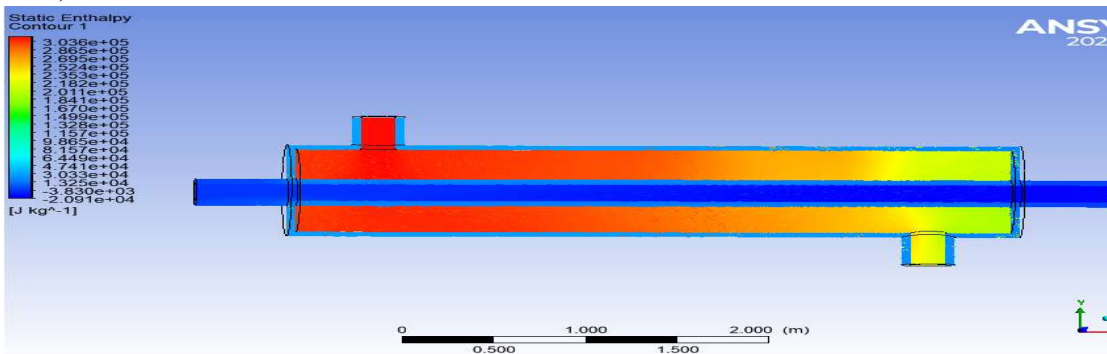
l) EG-TiO<sub>2</sub>



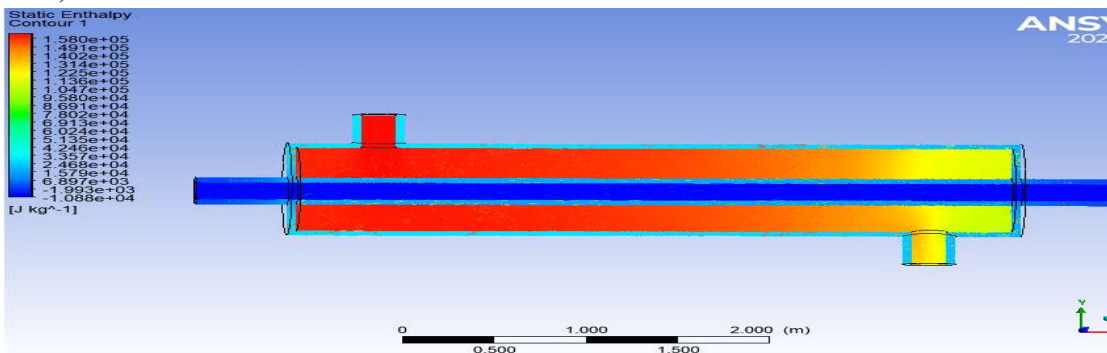
m) H<sub>2</sub>O-Al<sub>2</sub>O<sub>3</sub>



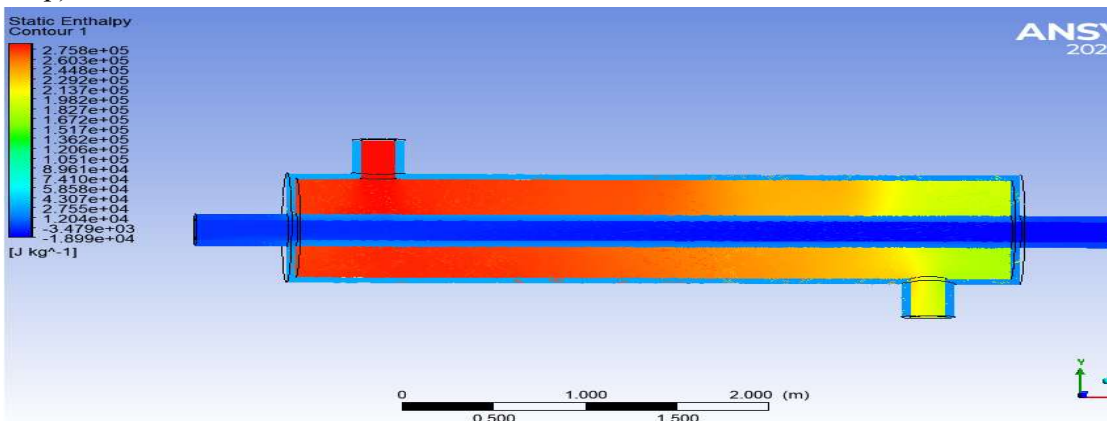
n) EG-Al<sub>2</sub>O<sub>3</sub>



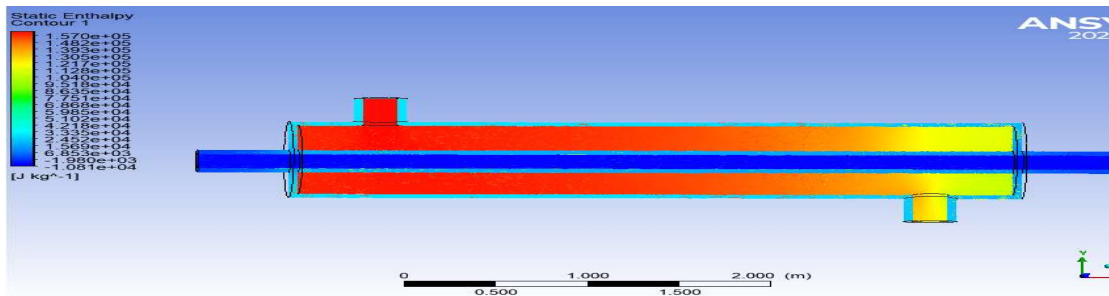
o) H<sub>2</sub>O-CuO



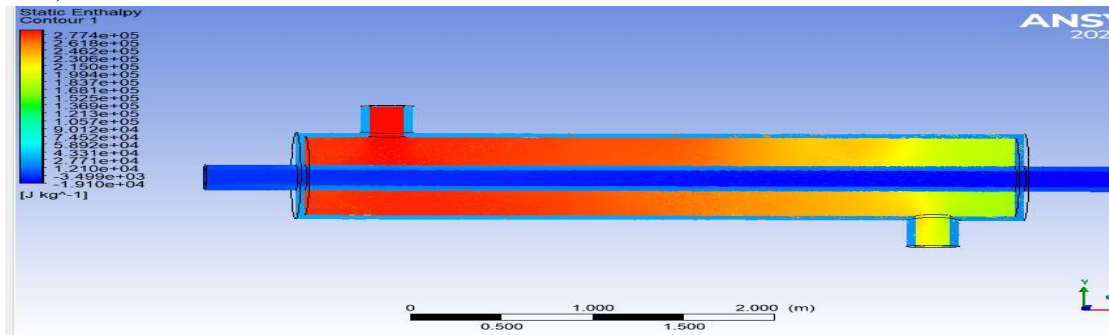
p) EG-CuO



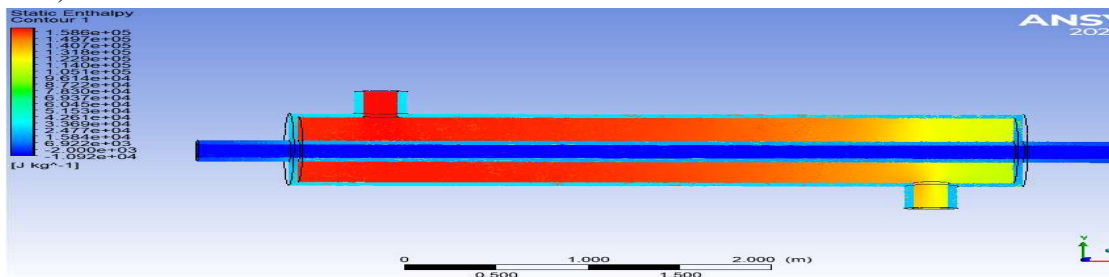
q) H<sub>2</sub>O-Cu



r) EG-Cu



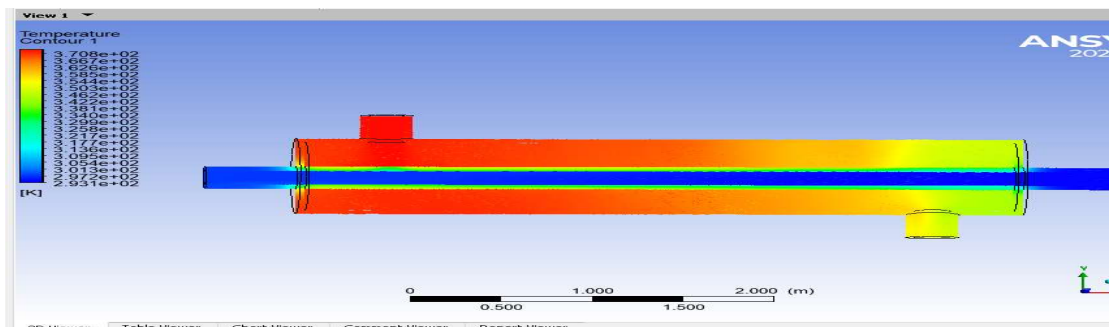
s) H<sub>2</sub>O-NiO



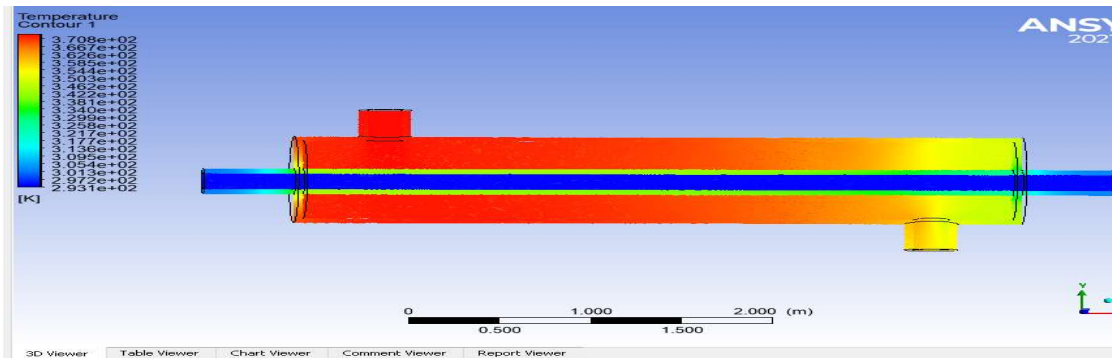
t) EG-NiO

**Figure 5.2: Enthalpy Drops at Exit for Different Materials**

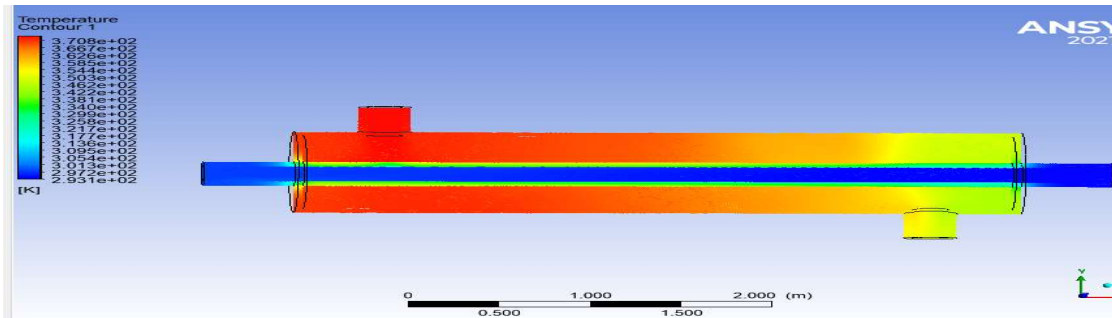
Figures 5.3 represents the results obtained for exit temperature.



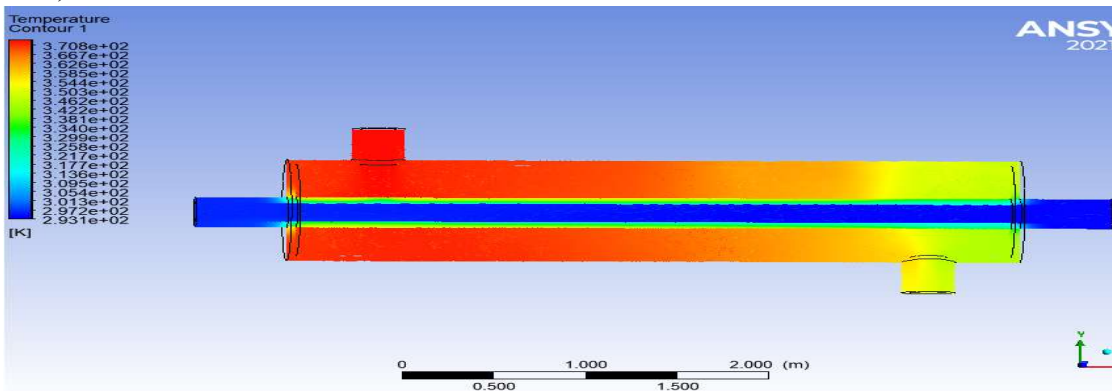
a) H<sub>2</sub>O-SiO<sub>2</sub>



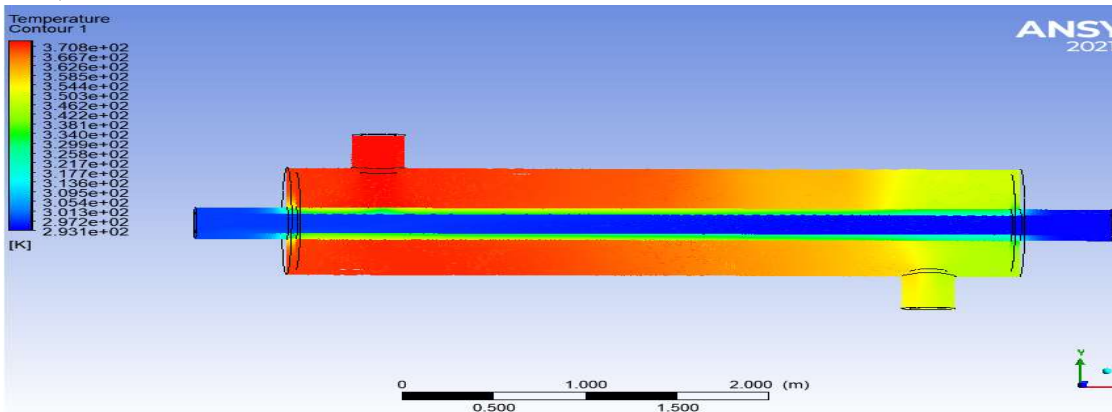
b) EG-SiO<sub>2</sub>



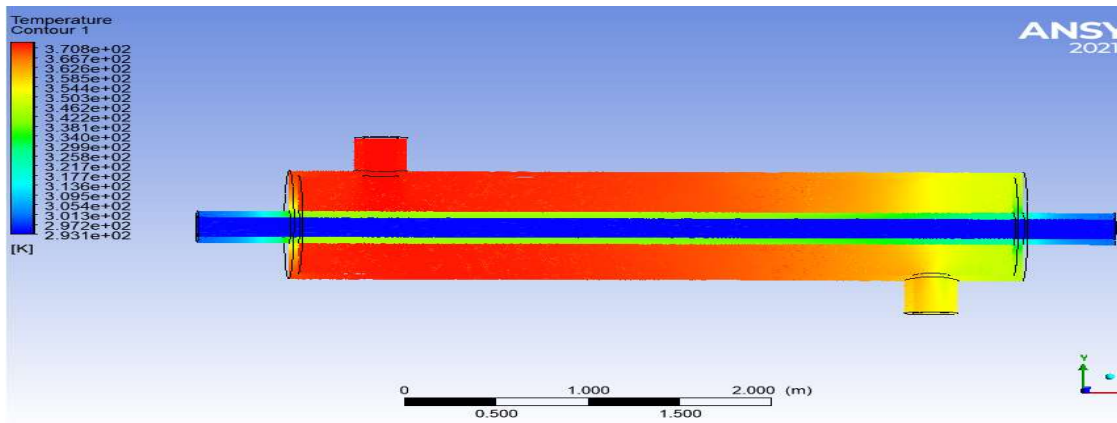
c) H<sub>2</sub>O-MVCNT



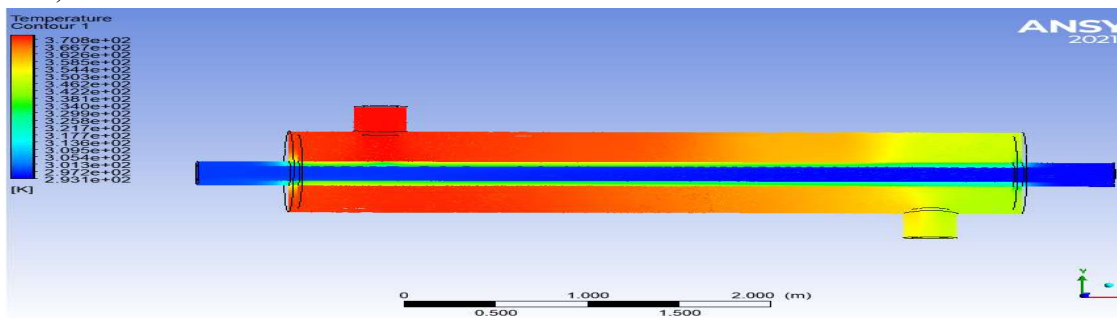
d) EG-MVCNT



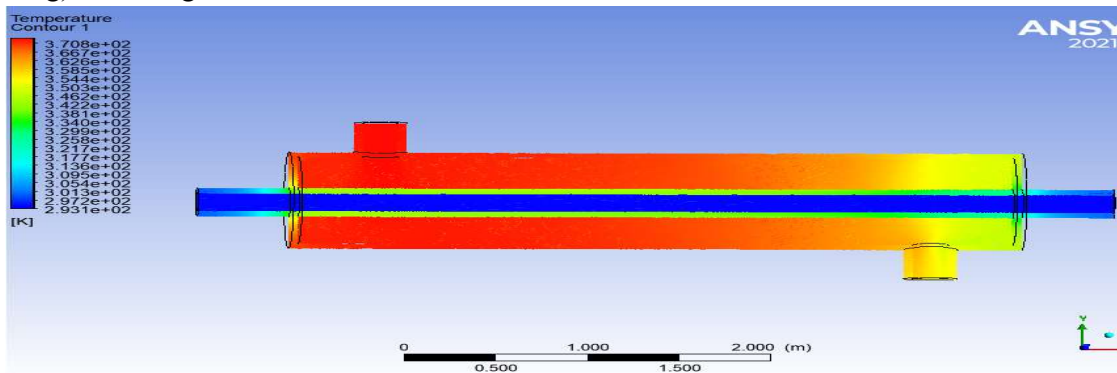
e) H<sub>2</sub>O-Al



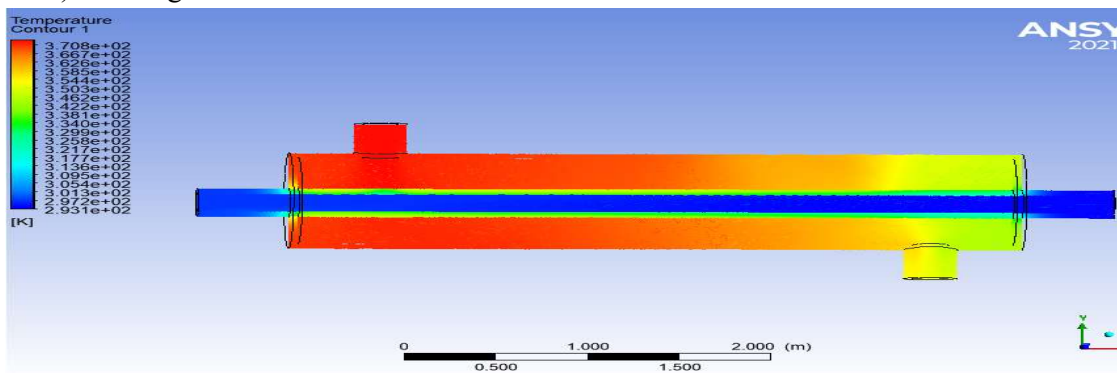
f) EG-Al



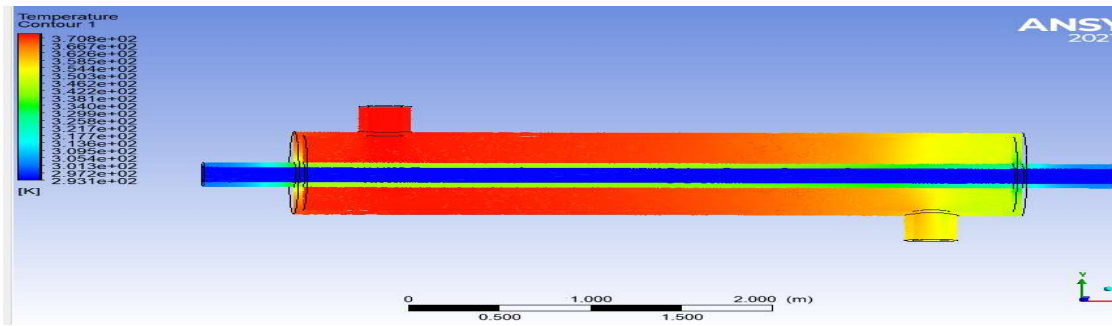
g) H<sub>2</sub>O-MgO



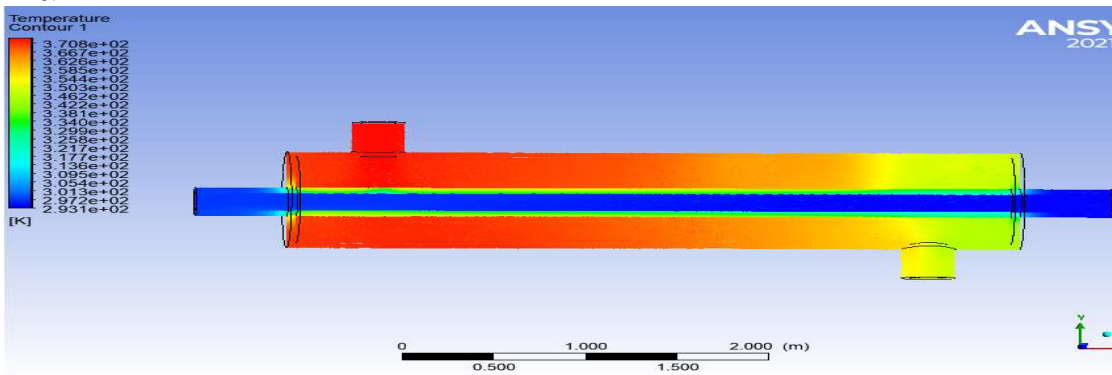
h) EG-MgO



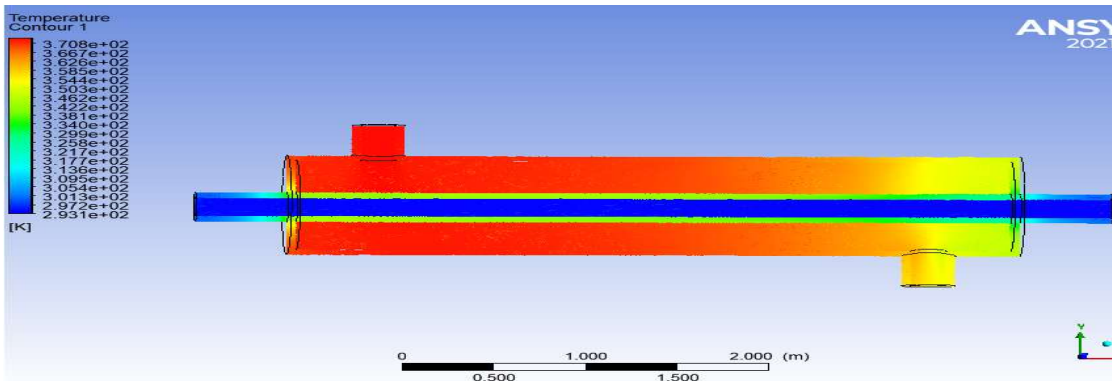
i) H<sub>2</sub>O



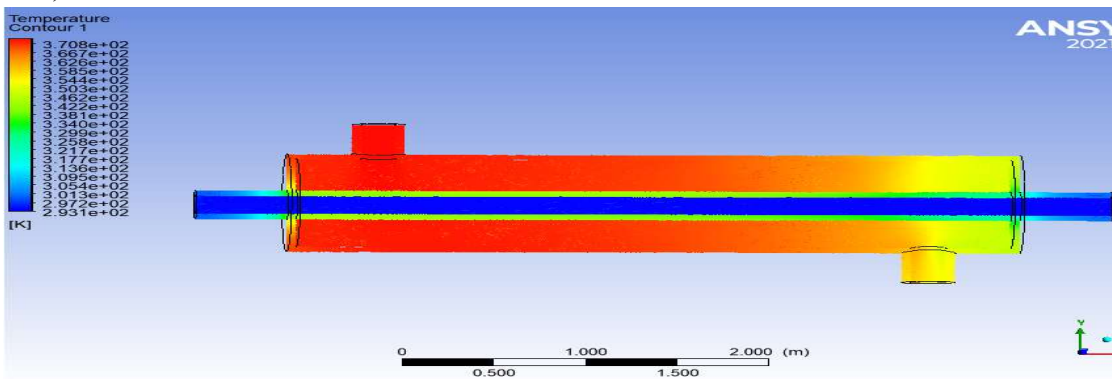
j) EG



k) H<sub>2</sub>O-TiO<sub>2</sub>

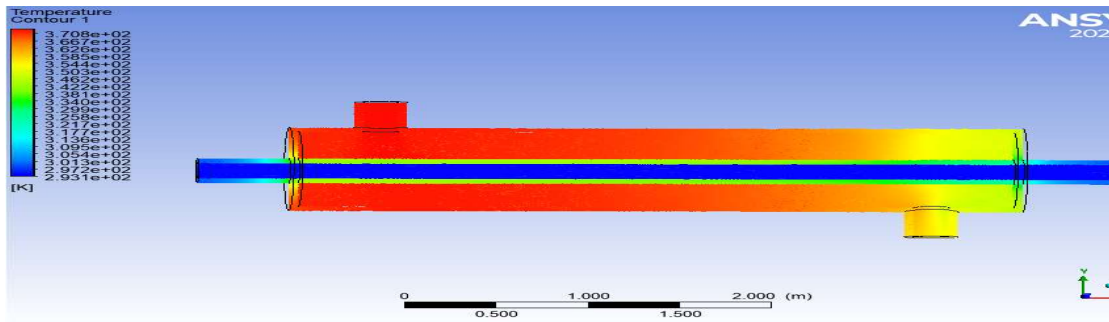


l) EG-TiO<sub>2</sub>

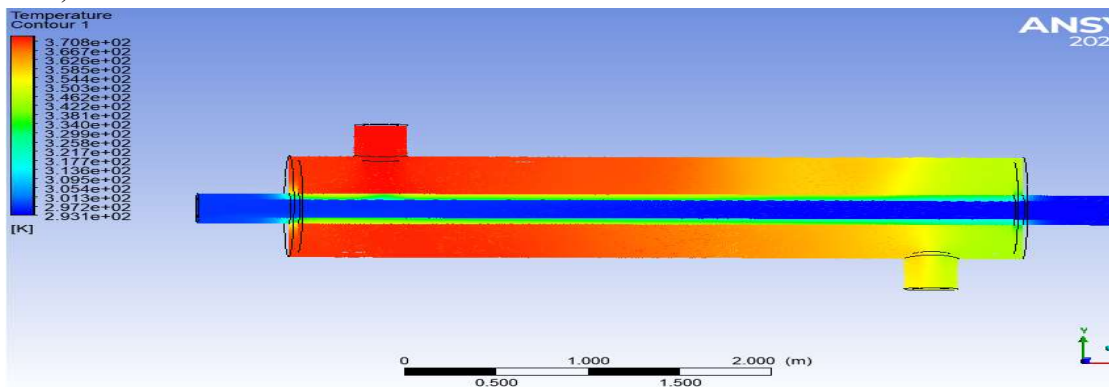


m) H<sub>2</sub>O-Al<sub>2</sub>O<sub>3</sub>

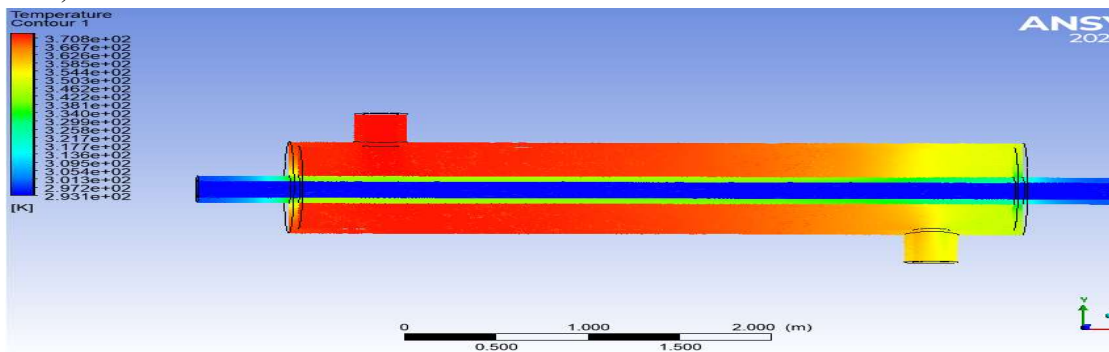




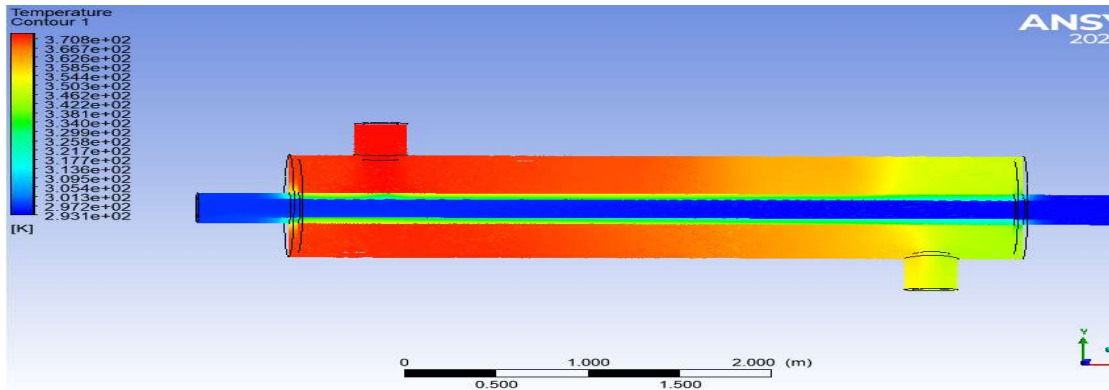
n) EG-Al<sub>2</sub>O<sub>3</sub>



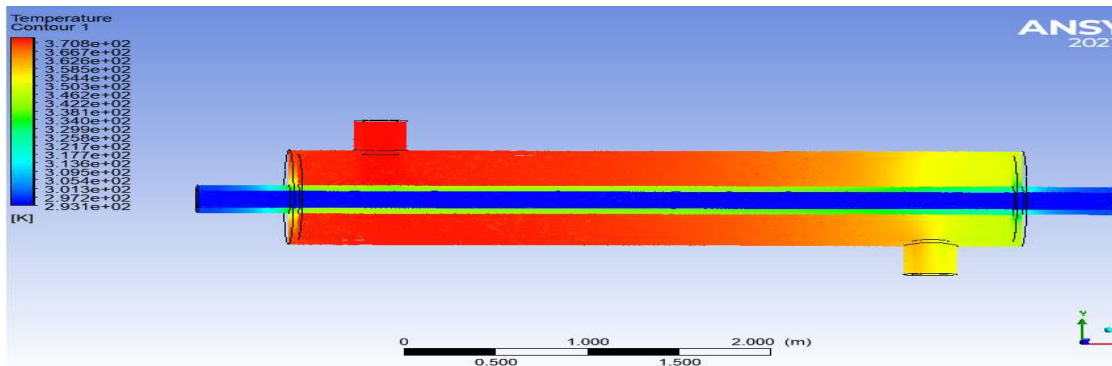
o) H<sub>2</sub>O-CuO



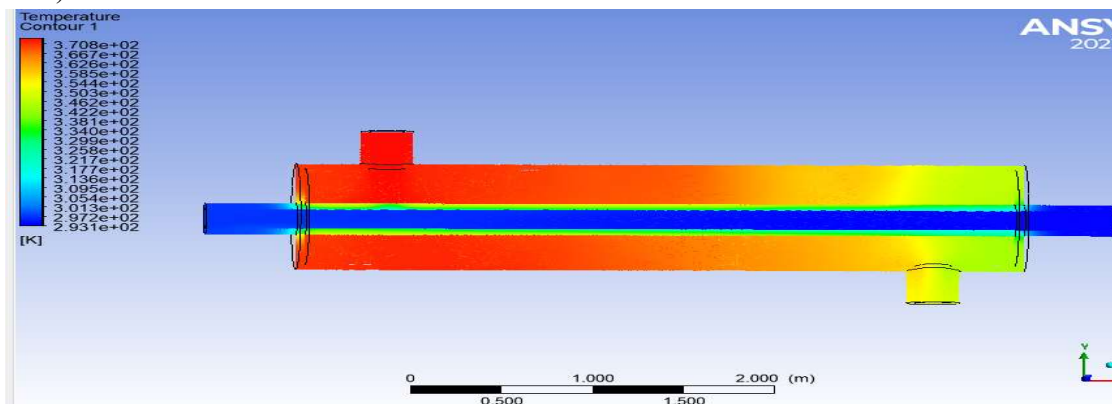
p) EG-CuO



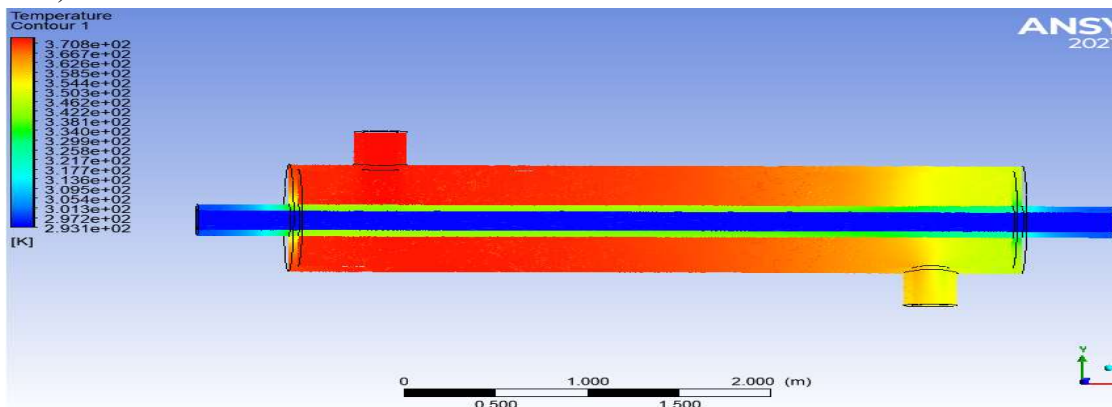
q) H<sub>2</sub>O-Cu



r) EG-Cu



s) H<sub>2</sub>O-NiO



t) EG-NiO

**Figure 5.3: Exit Temperatures for Different Materials**

## 5.2 Discussion

Figure 5.4 shows the details of maximum heat flux obtained for different alternatives as well as the rankings of materials.

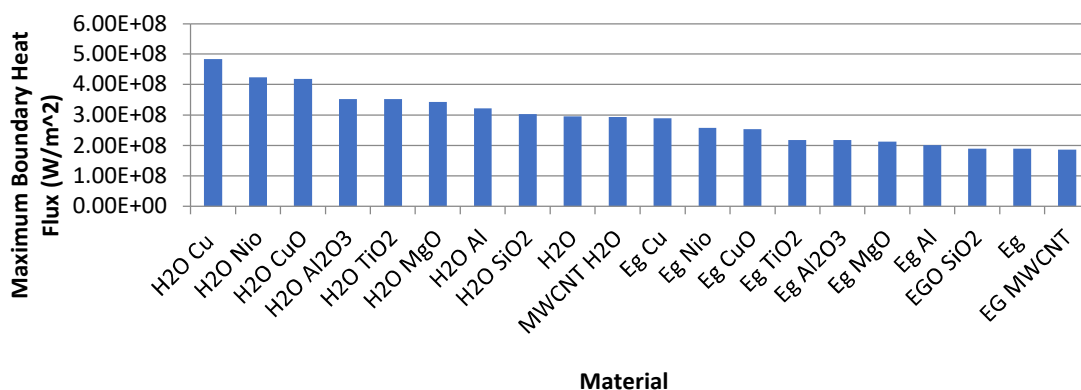


**Figure 5.4: Maximum Boundary Heat Flux for Different Alternatives**

Figure 5.4 shows that the combination of H<sub>2</sub>O-Cu shows the maximum value of heat flux, 4.83E+08 W/m<sup>2</sup>, and scores rank 1. In the similar manner the rank obtained by the combination H<sub>2</sub>O-NiO shows the rank 2 with the value of maximum heat flux as 4.24E+08 W/m<sup>2</sup>. Proceeding in the same manner, one can find that the nanofluid H<sub>2</sub>O-CuO scores rank 3 with the value of maximum heat flux is equal to 4.19E+08 W/m<sup>2</sup>. For rank 4 four alternatives, namely, A<sub>2</sub>O-Al<sub>2</sub>O<sub>3</sub> and H<sub>2</sub>O-TiO<sub>2</sub> appear, as they scored the value of maximum heat fluxes as 3.53E+08 W/m<sup>2</sup>. For rank 5, the nanofluid H<sub>2</sub>O-MgO seems to be suitable as it scores the value of maximum heat flux equals to 3.43E+08 W/m<sup>2</sup>. In the similar manner, the nanofluid H<sub>2</sub>O-Al scores heat flux equals to 3.22E+08 W/m<sup>2</sup>. For rank 7, the nanofluid H<sub>2</sub>O-SiO<sub>2</sub>, scores the value of heat flux equals to 3.04E+08 W/m<sup>2</sup>. Water appears at rank 8 with the value of heat flux equals to 2.96E+08 W/m<sup>2</sup>. At rank 19, the combination H<sub>2</sub>O-MWCNT appears with the heat flux value of 2.94E+08 W/m<sup>2</sup>, whereas the combination of ethylene glycol-copper appears at the rank 10 with the value of heat flux equals to 2.90E+08 W/m<sup>2</sup>.

Combination of ethylene glycol-NiO scores rank 11 with the value of heat flux equals to 2.58E+08 W/m<sup>2</sup>, whereas the alternative ethylene glycol-CuO obtains rank 12 with heat flux equals to 2.54E+08 W/m<sup>2</sup>. For rank 13, two alternatives, ethylene glycol-TiO<sub>2</sub> and ethylene glycol-al<sub>2</sub>O<sub>3</sub> appear with values of heat fluxes equal to 2.18E+08 W/m<sup>2</sup>. In the similar manner, the combination of ethylene glycol-MgO scores the rank 14 with heat flux value of 2.13E+08 W/m<sup>2</sup>. For rank 15 the combination of ethylene glycol-aluminum seems to be suitable with the value of maximum heat flux equals to 2.01E+08 W/m<sup>2</sup>. For rank 16, two alternatives, namely ethylene glycol-SiO<sub>2</sub> and ethylene glycol appear with the value of maximum heat flux equal to 1.90E+08 W/m<sup>2</sup>, and finally for rank 17, the alternative ethylene glycol-MWCNT appears with the maximum heat flux is equal to 1.86E+08 W/m<sup>2</sup>.

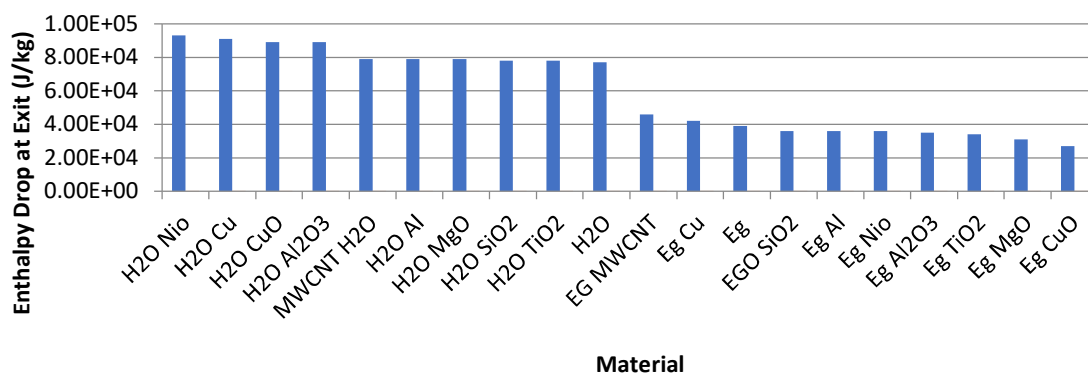


**Figure 5.5: Enthalpy Drop at Exit for Different Alternatives**

Figure 5.5 shows the values of exit enthalpy drops for different nanofluids, which in turn, describes their rankings for the criterion. It may be found that the alternative H<sub>2</sub>O-NiO scores the rank 1 with the enthalpy drop is equal to 9.30E+04 J/kg. Proceeding in the similar manner, for the rank 2, the alternative H<sub>2</sub>O-Cu with exit enthalpy drop of 9.10E+04 seems to be appropriate. For rank 3, two alternatives, namely H<sub>2</sub>O-CuO and H<sub>2</sub>O-Al<sub>2</sub>O<sub>3</sub> appear with the value of exit enthalpy drop equal to 8.90E+04 J/kg. Similarly, the 3 alternatives, namely H<sub>2</sub>O-MWCNT and H<sub>2</sub>O-Al and H<sub>2</sub>O-MgO appear at the rank 4 with exit enthalpy drop equals to 7.90E+04 J/kg. For rank 5, alternatives H<sub>2</sub>O-SiO<sub>2</sub> and H<sub>2</sub>O-TiO<sub>2</sub> appear with exit enthalpy drop equals to 7.80E+04 J/kg. Proceeding in the similar manner, for rank 6 water seems to be appropriate with the exit enthalpy drop of 7.70E+04 J/kg, and for rank 7, the alternative ethylene glycol-MWCNT seems to be appropriate with the value of exit enthalpy drop equals to 4.60E+04 J/kg.

For the rank 8, the alternative ethylene glycol-copper seems to be appropriate with the value of exit enthalpy drop equals to 4.20E+04 J/kg. For the rank 9, pure ethylene glycol secures the rank with exit enthalpy drop is equal to 3.90E+04 J/kg. For rank 10, three alternatives, namely ethylene glycol-SiO<sub>2</sub>, ethylene glycol-Al and ethylene glycol-NiO seem to be appropriate with the values of exit enthalpy drops equal to 3.60E+04 J/kg. Proceeding in the similar manner, for rank 11, the alternative ethylene glycol-Al<sub>2</sub>O<sub>3</sub> scores exit enthalpy drop of 3.50E+04 J/kg, for rank 12, the alternative ethylene glycol-TiO<sub>2</sub> scores the exit enthalpy drop of 3.40E+04 J/kg, for the rank 13, ethylene glycol-MgO scores exit enthalpy drop of 3.10E+04 J/kg and the last alternative, ethylene glycol-CuO appears at rank 14 with the exit enthalpy drop of 2.70E+04 J/kg.

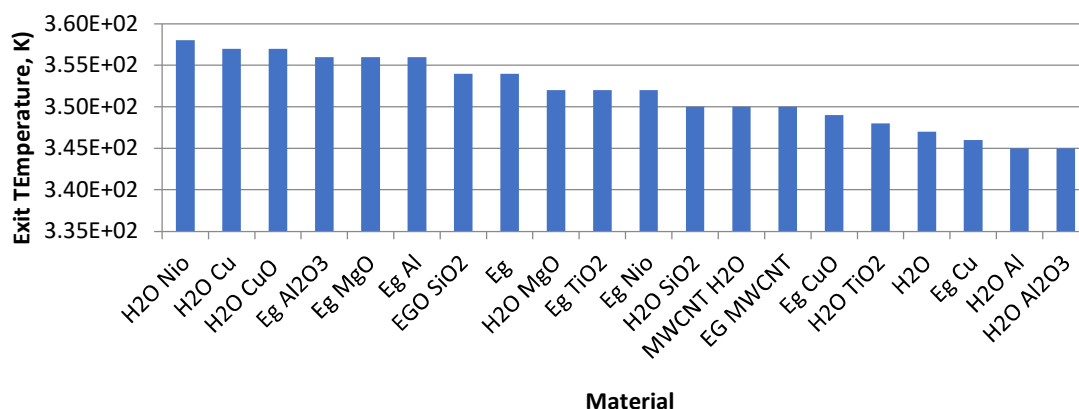


**Figure 5.6: Exit Temperatures for Different Alternatives**

Figure 5.6 shows the values of exit temperatures for different alternatives. The alternative H<sub>2</sub>O-NiO scores the rank 1, showing the maximum value of the exit temperature of 3.58E+02K. For rank 2, two alternatives namely H<sub>2</sub>O-Cu and H<sub>2</sub>O-CuO appear with the exit temperatures of 3.57E+02 K. Proceeding in the similar manner, for rank 3, three alternatives ethylene glycol-Al<sub>2</sub>O<sub>3</sub>, ethylene glycol-MgO and ethylene glycol-Al appear with the exit temperatures of 3.56E+02 K. Similarly, for the rank 4, two alternatives namely ethylene glycol-SiO<sub>2</sub> and pure ethylene glycol appear with the exit temperature of 3.54E+04 K, and for the rank 5, three alternatives, namely H<sub>2</sub>O-MgO, ethylene glycol-TiO<sub>2</sub> and ethylene glycol-NiO appear with the exit temperatures of 3.52E+02 K.

Proceeding in the similar manner, for rank 6, again three alternatives namely H<sub>2</sub>O-SiO<sub>2</sub>, H<sub>2</sub>O-MWCNT and ethylene glycol-MWCNT appear with the exit temperatures of 3.50E+02 K. For rank 7, alternative ethylene glycol-NiO appears with the exit temperature of 3.49E+02 K. For the rank 8, the alternative H<sub>2</sub>O-TiO<sub>2</sub> with the exit temperature of 3.48E+02 K seems to be appropriate. Water scores rank 9 with the exit temperature of 3.47E+02, whereas the alternative ethylene glycol-Cu scores rank 10 with the exit temperature of 3.46E+02 K. Finally, the alternative H<sub>2</sub>O-Al<sub>2</sub>O<sub>3</sub> scores rank 11 with the exit temperature value of 3.45E+02 K. Table 5.1 shows the rankings scored by different alternatives on different criteria.

**Table 5.1: Rankings of Alternatives on Different Criteria**

| S. No | Alternative                       | Criteria and Rankings                 |      |                              |      |                      |      |
|-------|-----------------------------------|---------------------------------------|------|------------------------------|------|----------------------|------|
|       |                                   | Maximum Heat Flux (W/m <sup>2</sup> ) | Rank | Enthalpy Drop at Exit (J/kg) | Rank | Exit Temperature (K) | Rank |
| 1.    | Eg                                | 1.90E+08                              | 16   | 3.90E+04                     | 9    | 3.54E+02             | 4    |
| 2.    | Eg-Al                             | 2.01E+08                              | 15   | 3.60E+04                     | 10   | 3.56E+02             | 3    |
| 3.    | Eg-Al <sub>2</sub> O <sub>3</sub> | 2.18E+08                              | 13   | 3.50E+04                     | 11   | 3.56E+02             | 3    |
| 4.    | Eg-Cu                             | 2.90E+08                              | 10   | 4.20E+04                     | 8    | 3.46E+02             | 10   |
| 5.    | Eg-CuO                            | 2.54E+08                              | 12   | 2.70E+04                     | 14   | 3.49E+02             | 7    |
| 6.    | Eg-MgO                            | 2.13E+08                              | 14   | 3.10E+04                     | 13   | 3.56E+02             | 3    |

|     |   |          |    |          |    |          |    |
|-----|---|----------|----|----------|----|----------|----|
| 7.  | Eg-MWCNT  | 1.86E+08 | 17 | 4.60E+04 | 7  | 3.50E+02 | 6  |
| 8.  | Eg-NiO  | 2.58E+08 | 11 | 3.60E+04 | 10 | 3.52E+02 | 5  |
| 9.  | Eg-SiO <sub>2</sub>                             | 1.90E+08 | 16 | 3.60E+04 | 10 | 3.54E+02 | 4  |
| 10. | Eg-TiO <sub>2</sub>                             | 2.18E+08 | 13 | 3.40E+04 | 12 | 3.52E+02 | 5  |
| 11. | H <sub>2</sub> O                                | 2.96E+08 | 8  | 7.70E+04 | 6  | 3.47E+02 | 9  |
| 12. | H <sub>2</sub> O-Al                             | 3.22E+08 | 6  | 7.90E+04 | 4  | 3.45E+02 | 11 |
| 13. | H <sub>2</sub> O-Al <sub>2</sub> O <sub>3</sub> | 3.53E+08 | 4  | 8.90E+04 | 3  | 3.45E+02 | 11 |
| 14. | H <sub>2</sub> O- Cu                            | 4.83E+08 | 1  | 9.10E+04 | 2  | 3.57E+02 | 2  |
| 15. | H <sub>2</sub> O-CuO                            | 4.19E+08 | 3  | 8.90E+04 | 3  | 3.57E+02 | 2  |
| 16. | H <sub>2</sub> O-MgO                            | 3.43E+08 | 5  | 7.90E+04 | 4  | 3.52E+02 | 5  |
| 17. | H <sub>2</sub> O-<br>MWCNT                      | 2.94E+08 | 9  | 7.90E+04 | 4  | 3.50E+02 | 6  |
| 18. | H <sub>2</sub> O-NiO                            | 4.24E+08 | 2  | 9.30E+04 | 1  | 3.58E+02 | 1  |
| 19. | H <sub>2</sub> O-SiO <sub>2</sub>               | 3.04E+08 | 7  | 7.80E+04 | 5  | 3.50E+02 | 6  |
| 20. | H <sub>2</sub> O-TiO <sub>2</sub>               | 3.53E+08 | 4  | 7.80E+04 | 5  | 3.48E+02 | 8  |

Figure 5.7 shows the above rankings in a graphical manner.

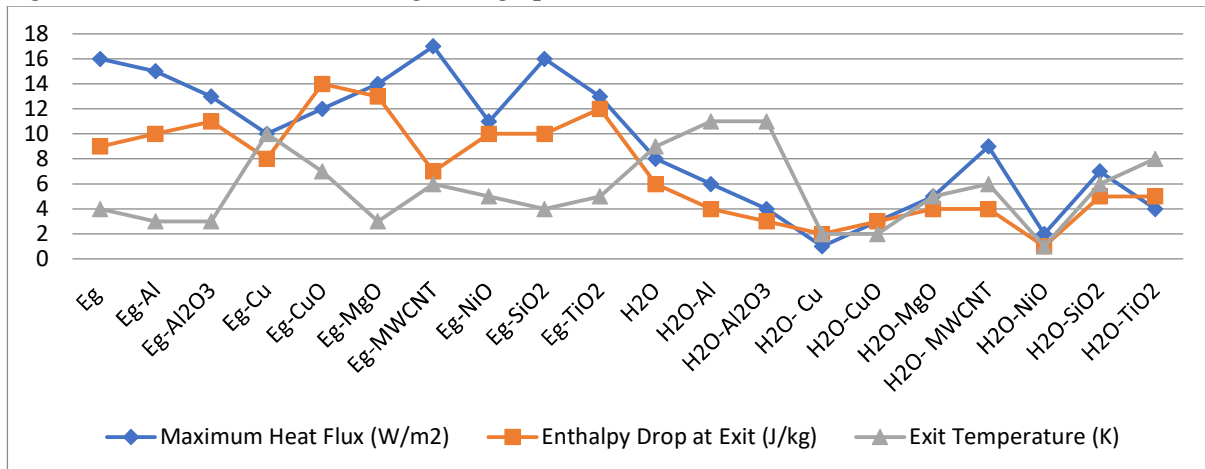


**Figure 5.7: Graphical Representation of Rankings of Alternatives on Different Criteria**

But, it may be found from the above analysis that there were significant variations in the rankings scored by different alternatives on the criteria maximum heat flux, and enthalpy drop at exit and exit temperature. It was also found that the difference in rankings scored by alternatives on criteria enthalpy drop at exit and exit temperature is more than that of maximum heat flux. So therefore, in order to get common rankings of alternatives, a statistical technique, relative standard deviation, which is defined as the percentage of ratio of standard deviation and average, was used, which yielded the following results. According to the concept or relative standard deviation, the criterion with the minimum value of relative standard deviation value was considered for the final ranking of alternatives.

**Table 5.2: Relative Standard Deviation for Different Criteria**

| S. No | Criteria              | Relative Standard Deviation | Remarks                                |
|-------|-----------------------|-----------------------------|--|
| 1.    | Maximum Heat Flux     | 29.680                      |  |
| 2.    | Enthalpy Drop at Exit | 41.510                      |  |
| 3.    | Exit Temperature      | 1.1960                      | <b>Preferred Criterion for Ranking</b> |

On the basis of above results, the criteria exit temperature was selected for the final ranking of alternatives, which may be verified by considering the working concept of the device that, which tells that maximum exit temperature for the hot fluid is necessary for the successful operation of an heat exchanger.

**Table 5.3: Overall Rankings of Alternatives**

| S. No | Alternatives                      | Exit Temperature (K) | Overall Rank |
|-------|-----------------------------------|----------------------|--------------|
| 1.    | H <sub>2</sub> O-NiO              | 3.58E+02             | 1            |
| 2.    | H <sub>2</sub> O- Cu              | 3.57E+02             | 2            |
| 3.    | H <sub>2</sub> O-CuO              | 3.57E+02             | 2            |
| 4.    | Eg-Al                             | 3.56E+02             | 3            |
| 5.    | Eg-Al <sub>2</sub> O <sub>3</sub> | 3.56E+02             | 3            |
| 6.    | Eg-MgO                            | 3.56E+02             | 3            |
| 7.    | Eg                                | 3.54E+02             | 4            |
| 8.    | Eg-SiO <sub>2</sub>               | 3.54E+02             | 4            |
| 9.    | Eg-NiO                            | 3.52E+02             | 5            |
| 10.   | Eg-TiO <sub>2</sub>               | 3.52E+02             | 5            |
| 11.   | H <sub>2</sub> O-MgO              | 3.52E+02             | 5            |
| 12.   | Eg-MWCNT                          | 3.50E+02             | 6            |
| 13.   | H <sub>2</sub> O- MWCNT           | 3.50E+02             | 6            |
| 14.   | H <sub>2</sub> O-SiO <sub>2</sub> | 3.50E+02             | 6            |
| 15.   | Eg-CuO                            | 3.49E+02             | 7            |
| 16.   | H <sub>2</sub> O-TiO <sub>2</sub> | 3.48E+02             | 8            |
| 17.   | H <sub>2</sub> O                  | 3.47E+02             | 9            |
| 18.   | Eg-Cu                             | 3.46E+02             | 10           |
| 19.   | H <sub>2</sub> O-Al               | 3.45E+02             | 11           |

|     |   |          |    |
|-----|---|----------|----|
| 20. | H <sub>2</sub> O-Al <sub>2</sub> O <sub>3</sub> | 3.45E+02 | 11 |
|-----|---|----------|----|

Figure 5.8 shows the graphical representation of Results.

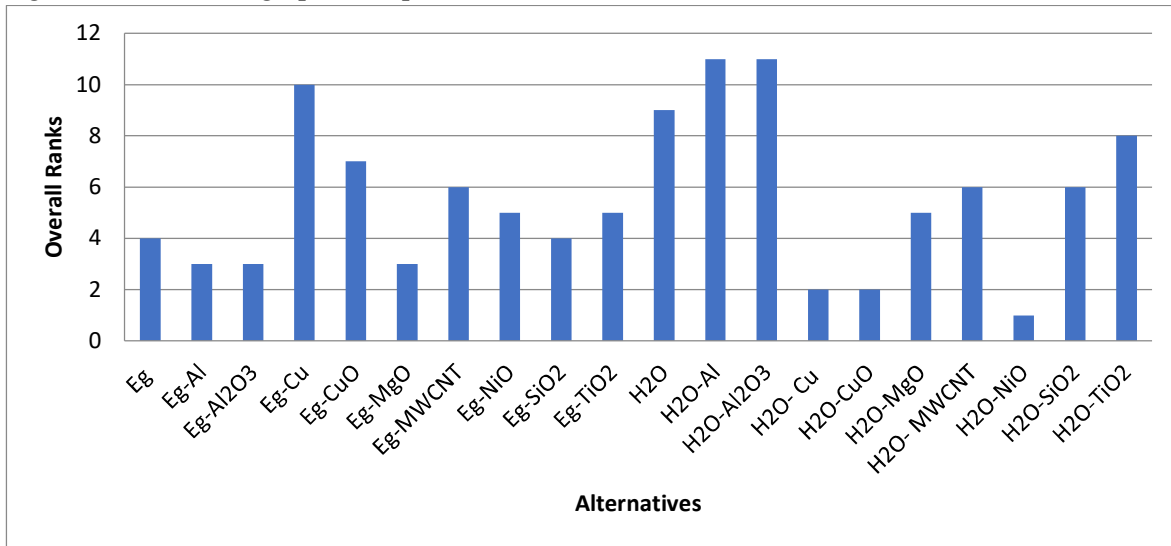


**Figure 5.8: Graphical Representation of Overall Ranking of Alternatives**

In this manner, overall ranking for the alternatives were obtained.

From the obtained results, water may be considered as the best alternative base fluid. It can also be found that yet the base fluid water has appeared at ranks 1 and 2, but most of the upper ranks are scored by ethylene glycol, and therefore its contribution cannot be neglected.

## 6. Conclusion, Limitations and Future Scope of the Research

Present section is devoted to the conclusion, limitations and future scope of the research work, the details of which are presented in upcoming sub-sections.

### 6.1 Conclusion

Present research work was based on the investigations on the application of different combinations of nanofluids and base fluids to a heat exchanger. For this purpose, ten types of nanoparticles were used with two base fluids, water and ethylene glycol with 10 percent volumetric concentration, and three thermal properties, namely, maximum heat flux, enthalpy drop at exit and temperature, were calculated. In the last step of research work, a statistical technique, relative standard deviation, was also employed to get a unique set of results. Following points represent the conclusion of the research work:

- The nanofluid H<sub>2</sub>O-NiO may be considered as the best alternative for the heat exchanger application; and
- H<sub>2</sub>O may be considered as the best base fluid for the heat exchanger application.

### 6.2 Limitations and Future Scope of the Research

Following points represent the limitations of the research:

- The research work is limited to a particular set of nano-particles;



- b) The research work is also limited to a particular concentration of nano fluids in base fluids; and
- c) The research work is limited to investigations on a particular set of thermal properties.

Based on above mentioned limitations, following points represent the future scope of the research work:

- a) A broader research work based on a broader set of nano-particles may be initiated;
- b) An extensive research work consisting a broader range of volumetric concentrations of nanoparticles may be initiated; and
- c) A broader research work, consisting of a broader set of thermal properties may be called.

### References and Web Resources

- Amanuel, T., & Mishra, M. (2018). Investigation of thermohydraulic performance of triple concentric-tube heat exchanger with CuO/water nanofluid: numerical approach. *Heat Transfer—Asian Research*, 47(8), 974-995.
- Anitha, S., Thomas, T., Parthiban, V., & Pichumani, M. (2019). What dominates heat transfer performance of hybrid nanofluid in single pass shell and tube heat exchanger?. *Advanced Powder Technology*, 30(12), 3107-3117.
- Arulprakasajothi, M., Elangovan, K., Chandrasekhar, U., & Suresh, S. (2018). Performance study of conical strip inserts in tube heat exchanger using water based titanium oxide nanofluid. *Thermal Science*, 22(1 Part B), 477-485.
- Barzegarian, R., Aloueyan, A., & Yousefi, T. (2017). Thermal performance augmentation using water based Al<sub>2</sub>O<sub>3</sub>-gamma nanofluid in a horizontal shell and tube heat exchanger under forced circulation. *International Communications in Heat and Mass Transfer*, 86, 52-59.
- Bhanvase, B. A., Sayankar, S. D., Kapre, A., Fule, P. J., & Sonawane, S. H. (2018). Experimental investigation on intensified convective heat transfer coefficient of water based PANI nanofluid in vertical helical coiled heat exchanger. *Applied thermal engineering*, 128, 134-140.
- Bhattad, A., Sarkar, J., & Ghosh, P. (2020). Heat transfer characteristics of plate heat exchanger using hybrid nanofluids: effect of nanoparticle mixture ratio. *Heat and Mass Transfer*, 56(8), 2457-2472.
- Chaurasia, S. R., & Sarviya, R. M. (2020). Thermal performance analysis of CuO/water nanofluid flow in a pipe with single and double strip helical screw tape. *Applied Thermal Engineering*, 166, 114631.
- Chupradit, S., Jalil, A. T., Enina, Y., Neganov, D. A., Alhassan, M. S., Aravindhan, S., & Davarpanah, A. (2021). Use of Organic and Copper-Based Nanoparticles on the Turbulator Installment in a Shell Tube Heat Exchanger: A CFD-Based Simulation Approach by Using Nanofluids. *Journal of Nanomaterials*, 2021.
- Ghozatloo, A., Rashidi, A., & Shariaty-Niassar, M. (2021). Convective heat transfer enhancement of graphene nanofluids in shell and tube heat exchanger. *Experimental Thermal and Fluid Science*, 53, 136-141.

- Gugulothu, R., Reddy, K. V. K., Somanchi, N. S., & Adithya, E. L. (2017a). A review on enhancement of heat transfer techniques. *Materials Today: Proceedings*, 4(2), 1051-1056.
- Gugulothu, R., Somanchi, N. S., Reddy, K. V. K., & Akkiraju, K. (2017b). A review on enhancement of heat transfer in heat exchanger with different inserts. *Materials today: proceedings*, 4(2), 1045-1050.
- Issa, R. J. (2021). A Review on Thermophysical Properties and Nusselt Number Behavior of Al<sub>2</sub>O<sub>3</sub> Nanofluids in Heat Exchangers. *Journal of Thermal Science*, 1-14.
- Kanti, P., Sharma, K. V., Ramachandra, C. G., & Panitapu, B. (2020). Stability and thermophysical properties of fly ash nanofluid for heat transfer applications. *Heat Transfer*, 49(8), 4722-4737.
- Kleinstreuer, C., & Feng, Y. (2011). Experimental and theoretical studies of nanofluid thermal conductivity enhancement: a review. *Nanoscale research letters*, 6(1), 1-13.
- Malika, M., Bhad, R., & Sonawane, S. S. (2021). ANSYS simulation study of a low volume fraction CuO–ZnO/water hybrid nanofluid in a shell and tube heat exchanger. *Journal of the Indian Chemical Society*, 98(11), 100200.
- Manikandan, S. P., & Baskar, R. (2018). Heat transfer studies in compact heat exchanger using ZnO and TiO<sub>2</sub> nanofluids in ethylene glycol/water. *Chemical Industry and Chemical Engineering Quarterly*, 24(4), 309-318.
- Naik, B. A. K., & Vinod, A. V. (2018). Heat transfer enhancement using non-Newtonian nanofluids in a shell and helical coil heat exchanger. *Experimental Thermal and Fluid Science*, 90, 132-142.
- Nivedini, G., Prasad, K., Sandeep, C., & Rao, K. V. (2020). Empirical and CFD analysis of silica nanofluid using a double pipe heat exchanger. *SN Applied Sciences*, 2(12), 1-10.
- Nivedini, G., Prasad, K., Sandeep, C., & Venkateswara Rao, K. (2020). Empirical and CFD analysis of silica nanofluid using a double pipe heat exchanger. *SN Applied Sciences*, 2(12), 1-10.
- Palanisamy, K., & Mukesh Kumar, P. C. (2017). Heat transfer enhancement and pressure drop analysis of a cone helical coiled tube heat exchanger using MWCNT/water nanofluid. *Journal of Applied Fluid Mechanics*, 10(Special Issue), 7-13.
- Purbia, D., Khandelwal, A., Kumar, A., & Sharma, A. K. (2019). Graphene-water nanofluid in heat exchanger: mathematical modelling, simulation and economic evaluation. *International Communications in Heat and Mass Transfer*, 108, 104327.
- Puspitasari, F. H., Salamah, U., Sari, N. R., Maddu, A., & Solikhin, A. (2020). Potential of Chitosan Hydrogel Based Activated Carbon Nanoparticles and Non-Activated Carbon Nanoparticles for Water Purification. *Fibers and Polymers*, 21(4), 701-708.
- Radkar, R. N., Bhanvase, B. A., Barai, D. P., & Sonawane, S. H. (2019). Intensified convective heat transfer using ZnO nanofluids in heat exchanger with helical coiled geometry at constant wall temperature. *Materials Science for Energy Technologies*, 2(2), 161-170.
- Rajput, N. S., Shukla, D. D., Ishan, L., & Madhav, K. S. (2021). Enhancement of Nusselt number by using Al<sub>2</sub>O<sub>3</sub> and TiO<sub>2</sub> Nanofluids in Heat Exchangers. *Materials Today: Proceedings*, 47, 6515-6521.

- Rao, V. N., & Sankar, B. R. (2019). Heat transfer and friction factor investigations of CuO nanofluid flow in a double pipe U-bend heat exchanger. *Materials Today: Proceedings*, 18, 207-218.
- Reddy, M. M., Praveen, L., & Srinivas, A. (2021, February). Thermal analysis of shell and tube heat exchangers for improving heat transfer rate using nanofluid mixtures. In *AIP Conference Proceedings* (Vol. 2317, No. 1, p. 030029). AIP Publishing LLC.
- Salari, M., Assari, M. R., Ghafouri, A., & Pourmahmoud, N. (2020). Experimental study on forced convection heat transfer of a nanofluid in a heat exchanger filled partially porous material. *Journal of Thermal Analysis and Calorimetry*, 1-15.
- Sathish, T., Muthukumar, K., Saravanan, R., & Dhinakaran, V. (2020, October). Study on temperature difference of aluminium nitride nanofluid used in solar flat plate collector over normal water. In *AIP Conference Proceedings* (Vol. 2283, No. 1, p. 020126). AIP Publishing LLC.
- Sharma, S. K., Gupta, S. M., & Kumar, A. (2017). Hydrodynamic studies of CNT nanofluids in helical coil heat exchanger. *Materials Research Express*, 4(12), 124002.
- Singh, S. K., & Sarkar, J. (2020). Improvement in energy performance of tubular heat exchangers using nanofluids: A review. *Current Nanoscience*, 16(2), 136-156.
- Somasekhar, K., Rao, K. M., Sankararao, V., Mohammed, R., Veerendra, M., & Venkateswararao, T. (2018). A CFD investigation of heat transfer enhancement of shell and tube heat exchanger using Al<sub>2</sub>O<sub>3</sub>-water nanofluid. *Materials Today: Proceedings*, 5(1), 1057-1062.
- Sundar, L. S., Kumar, N. R., Addis, B. M., Bhramara, P., Singh, M. K., & Sousa, A. C. (2019). Heat transfer and effectiveness experimentally-based analysis of wire coil with core-rod inserted in Fe<sub>3</sub>O<sub>4</sub>/water nanofluid flow in a double pipe U-bend heat exchanger. *International Journal of Heat and Mass Transfer*, 134, 405-419.
- Thakur, G., & Singh, G. (2017). An experimental investigation of heat transfer characteristics of water based Al<sub>2</sub>O<sub>3</sub> nanofluid operated shell and tube heat exchanger with air bubble injection technique. *International Journal of Engineering & Technology*, 6(4), 83-90.
- Thakur, G., Singh, G., Thakur, M., & Kajla, S. (2018). An experimental study of nanofluids operated shell and tube heat exchanger with air bubble injection. *International Journal of Engineering*, 31(1), 136-143.
- [www.scholar.google.com](http://www.scholar.google.com)